IMA Journal of Mathematical Control and Information (2025) **42**, 1–34
https://doi.org/10.1093/imamci/dnaf027

Event-triggered PDE-based control of freeway traffic flow with connected/automated vehicles

Xinyong Wang
College of Control Science and Engineering, Bohai University, Jinzhou, 121013, China

Ying Tang, Nicolas Espitia*
Univ. Lille, CNRS, Centrale Lille, UMR 9189 CRIStAL, F-59000 Lille, France
*Corresponding author. Email: nicolas.espitia-hoyos@univ-lille.fr

AND

Nikolaos Bekiaris-Liberis
Department of Electrical and Computer Engineering, Technical University of Crete, G-73100 Chania, Greece

[Received on 11 February 2025; revised on 26 May 2025; accepted on 19 August 2025]

This paper addresses the event-triggered control problem for a modified Aw–Rascle–Zhang (ARZ) traffic model under congestion conditions. The considered ARZ-type model, described by non-linear first-order hyperbolic partial differential equations, represents traffic flow involving both adaptive cruise control-equipped (ACC-equipped) vehicles and human-driven vehicles. The control inputs are time-gap settings for ACC-equipped vehicles that are updated based on a suitable event-triggering condition. For the linearized and transformed system (a 2×2 linear hyperbolic system with in-domain control and dynamic boundary condition), we provide input-to-state stability estimates (in the sup-norm) with respect to actuation errors. Based on a small-gain approach, we design an appropriate triggering rule (yielding small-gain-based event triggering condition). We ensure the exponential stability in the sup-norm of the closed-loop system and Zeno-free behaviour. Numerical simulations illustrate the efficiency of the proposed control strategy in stabilizing traffic flow.

Keywords: event-triggered control; ARZ traffic model; first-order hyperbolic PDE; small-gain approach.

1. Introduction

The control of traffic flow on highways has been an important research focus over the past decades. While many different control strategies have been explored, we list here only some examples of the existing works. For example, in Papageorgiou (1980), the author proposes a time-of-day control strategy by considering the evolution of traffic flow according to the time delay between a volume change at a ramp and the subsequent disturbance at a freeway point downstream. Integrated control strategies for arbitrary topology traffic corridors, including motorways and signal-controlled urban roads, were presented in Papageorgiou (1995). In Bayen *et al.* (2022), control problems of vehicular traffic were studied based on conservation laws. The boundary controller was provided for a traffic flow model, while the velocity of the dynamics depends on a weighted average of the traffic density ahead in Bayen *et al.* (2021). In Goatin *et al.* (2016), the authors investigate the integration of variable speed limits and coordinated ramp metering within the framework of the traffic flow networks.

Various mathematical models have been proposed for traffic flow, such as the Payne–Whitham model (Payne, 1971), which describes non-equilibrium traffic flows, the Lighthill–Whitham–Richards model (Whitham, 1974), where the traffic is restricted to equilibrium states, the Aw–Rascle–Zhang (ARZ) model (combining the Aw–Rascle framework (Aw & Rascle, 2000) with Zhang's non-equilibrium extension (Zhang, 2002)), along with their numerous variations. Among these models, the ARZ model has gained particular attention due to its ability to capture the complex relationship between vehicle density and velocity (Yu & Krstic, 2019).

With the integration of adaptive cruise control (ACC)-equipped (Yu & Wang, 2022) and connected automated vehicles (Li *et al.*, 2023), the challenge of managing traffic flow in mixed environments involving both human-driven and ACC-equipped vehicles becomes more critical. Some research works have attempted to address this challenge, for example, the delay-compensated control for freeway traffic with connected vehicles (Qi *et al.*, 2023), the elimination of bistability and phantom traffic jams in mixed traffic systems (Molnar & Orosz, 2024) and the safety of connected automated vehicles employing connected cruise control (Chen *et al.*, 2024), as well as novel schemes that integrate a performance-based controller with a safety-oriented controller (Alan *et al.* (2023)) enabling compatibility with a wide range of controllers while ensuring instantaneous operation. The boundary stabilization problem for mixed traffic on freeways, where traffic dynamics are modelled as uncertain coupled hyperbolic partial differential equations (PDEs) with Markov jumping parameters, has been addressed in Zhang *et al.* (2024). However, traditional control approaches may impose limitations in terms of communication and computational load, particularly under mixed traffic conditions.

Event-triggered control (ETC) has recently emerged as an effective approach to address these limitations by reducing the frequency of control updates while maintaining system stability (Heemels *et al.*, 2012).

Unlike traditional time-triggered systems, ETC applies the control input only when certain conditions are satisfied, which can lead to significant savings in communication and computation (Tabuada, 2007). This strategy has shown promising results for PDE systems, including one-dimensional hyperbolic systems (linear, semi-linear and non-linear hyperbolic PDEs); see e.g. Espitia *et al.* (2016, 2018); Espitia (2020); Diagne & Karafyllis (2021) and Strecker *et al.* (2024), and one-dimensional parabolic systems; see e.g. Selivanov & Fridman (2016); Espitia *et al.* (2021); Katz *et al.* (2021); Rathnayake *et al.* (2021) and Rathnayake *et al.* (2024) among others. Event-triggered rules are also studied for coupled PDE–ordinary differential equation (ODE) systems (Wang & Krstic, 2021) and PDE–PDE systems (Koudohode *et al.*, 2024). Recently, the ETC has been investigated for stabilizing traffic flow, using PDE-backstepping approach (Espitia *et al.*, 2020). Subsequently, an event-triggered output-feedback control based on backstepping method is proposed to stabilize the traffic flow on two connected roads described by coupled hyperbolic PDEs (Espitia *et al.*, 2022). More advanced and notable recent contributions deal with event-triggered PDE backstepping in conjunction with performance-barrier strategies for not only reducing the stop-and-go traffic flow but also with larger inter-execution times; see e.g. Zhang *et al.* (2025). In Zhang & Yu (2024), an event-triggered boundary control framework for mixed-autonomy traffic systems modelled by hyperbolic PDEs was provided, capturing the dynamics of human-driven and autonomous vehicles, as well as their interactions. However, there is still limited research on ETC strategies for traffic.

Building on the recent work of Bekiaris-Liberis & Delis (2021), which introduces an ARZ-type model for traffic flow consisting of both human-driven and ACC-equipped vehicles, and develops a Lyapunov-based continuous control design, we extend this framework by introducing an ETC scheme to stabilize traffic flow governed by a mixed-traffic ARZ model while updating control actions—adjusting the time gap for ACC-equipped vehicles—based on a suitable small-gain based triggering rule. We

perform the stability analysis on a linearized and transformed ARZ model (a 2×2 linear hyperbolic system with in-domain control and dynamic boundary condition) and provide input-to-state stability (ISS) estimates with respect to actuation errors. A small-gain approach (Karafyllis & Krstic, 2018; Espitia *et al.*, 2021; Karafyllis & Krstic, 2021) is employed to design the suitable triggering rule (small-gain-based event- triggering condition). The small-gain condition drives the selection of the triggering parameters. With the help of small-gain arguments, we obtain estimates of the closed-loop system. We prove the avoidance of the Zeno phenomenon, which allows us to conclude the exponential stability result, though we highlight that the lower bounds of the inter-execution times turn out not to be uniform. Nevertheless, we also point out a natural extension of our ETC strategy to a *Self-triggered Control (STC)* strategy, which suggests that the next triggering time is predicted based on the current state information at the current sampled time. The main contributions of this paper are summarized as follows:

- We develop an ETC strategy for the ARZ traffic model that includes both ACC-equipped and manually driven vehicles.
- We establish the ISS estimates of the closed-loop system and use small-gain arguments to design an appropriate triggering rule.
- We provide the exponential stability under the proposed ETC strategy and demonstrate the avoidance of Zeno behaviour.
- We outline a possible STC strategy for traffic flow control.

Compared with the preliminary version of this work (Wang *et al.*, 2025), in the present paper, we extend the theoretical analysis by providing detailed proofs and conducting an in-depth analysis. In addition, we enhance the simulation part by providing the number of events in the event-triggered mechanism obtained at different small gain parameters.

The structure of this paper is as follows: Section 2 introduces the ARZ traffic model and the formulation of the problem. Section 3 discusses how nominal control is emulated by an ETC approach and presents the main results, which include the analysis of stability using the ETC based on small-gain conditions and the analysis to avoid the Zeno phenomenon. Section 4 presents numerical simulations that illustrate the performance of the ETC in stabilizing traffic flow. Finally, Section 5 a concludes the paper and outlines future research directions.

Notation. $\mathbb{R}_+$ will denote the set of non-negative real numbers. Let $S \subseteq \mathbb{R}^n$ be an open set and let $A \subseteq \mathbb{R}^n$ be an open set that satisfies $S \subseteq A \subseteq \bar{S}$. By $\mathscr{C}^0(A;\Omega)$, we denote the class of continuous functions on A, which take values in $\Omega \subseteq \mathbb{R}$. By $\mathscr{C}^k(A;\Omega)$, where $k \geq 1$ is an integer, we denote the class of functions on A, which takes values in Ω and has continuous derivatives of order k. For any integer $p > 0$, we denote $L^p([0,1],\mathbb{R})$ the space of real-valued p-integrable functions defined on $[0,1]$ with the standard L^p norm, i.e. for any $f \in L^p([0,1],\mathbb{R})$, we have $||f||_{L^p} := \left(\int_0^1 |f(x)|^p dx\right)^{\frac{1}{p}}$. We denote $\|f\|_\infty = \max_{x\in[0,1]} |f(x)| = \lim_{p\to\infty} \|f\|_{L^p}$. Let $u : \mathbb{R}_+ \times [0,1] \to \mathbb{R}$ be given. $u(t,\cdot)$ denotes the profile of u at certain $t \geq 0$, for all $x \in [0,1]$.

2. System description and problem formulation

The ARZ model is a traffic flow model based on PDEs. It is mainly used to describe the dynamic characteristics of traffic density and speed, and can capture some important phenomena in traffic flow,

such as 'stop-and-go' fluctuations and sudden drops in traffic volume. This model is instrumental in analysing and controlling traffic congestion.

2.1. *ARZ type traffic flow model with mixed vehicles*

The ARZ model, originally developed for human-driven vehicles (Aw & Rascle, 2000; Zhang, 2002), can be extended to accommodate mixed traffic environments containing human-driven and ACC-equipped vehicles. The traffic flow can be regulated by introducing time-gap control variables. In this case, the model uses a mixed speed equation (that we will denote by V_{mix} in the sequel) to combine ACC-equipped and human-driven vehicles' response characteristics into a common speed expression.

We consider the following model, which can be seen as a modification of the ARZ traffic model as presented in Bekiaris-Liberis & Delis (2021):

$$\rho_t(t,\bar{x}) = -\rho_{\bar{x}}(t,\bar{x})v(t,\bar{x}) - \rho(t,\bar{x})v_{\bar{x}}(t,\bar{x}), \tag{2.1}$$

$$\begin{aligned} v_t(t,\bar{x}) = &-\rho(t,\bar{x})\frac{\partial V_{\text{mix}}\left(\rho(t,\bar{x}),h_{\text{acc}}(t,\bar{x})\right)}{\partial\rho}v_{\bar{x}}(t,\bar{x}) - v(t,\bar{x})v_{\bar{x}}(t,\bar{x}) \\ &+\frac{V_{\text{mix}}\left(\rho(t,\bar{x}),h_{\text{acc}}(t,\bar{x})\right)-v(t,\bar{x})}{\tau_{\text{mix}}}, \end{aligned} \tag{2.2}$$

$$\rho(t,0) = q_{\text{in}}/v(t,0), \tag{2.3}$$

$$v_t(t,L) = \frac{V_{\text{mix}}\left(\rho(t,L),h_{\text{acc}}(t,L)\right)-v(t,L)}{\tau_{\text{mix}}}. \tag{2.4}$$

Here, $\rho(t,\bar{x})$ represents the traffic density (vehicles per unit length), and $v(t,\bar{x})$ denotes the average speed of vehicles. These variables are defined over the domain $(t,\bar{x}) \in \mathbb{R}_+ \times [0,L]$, where t represents time, $\bar{x}$ is the spatial coordinate. The spatio-temporal-dependent time-gap setting $h_{\text{acc}}(t,\bar{x})$ of ACC-equipped vehicles is considered as a control input that determines the desired spacing behaviour of ACC-equipped vehicles at time t and location $\bar{x}$. The traffic parameters involved in the model (2.1)–(2.4) are described in Table 1.

The traffic density equation (2.1) represents the conservation of vehicles, that is, the number of vehicles per unit length of road remains unchanged. The speed equation (2.2) describes the dynamic changes of traffic speed based on the relationship between traffic density and expected speed. Equation (2.3) describes the boundary condition of traffic density at the inlet of the considered freeway stretch (i.e. at $\bar{x} = 0$). This boundary condition reflects the impact of the external inflow q_{in} on the traffic density entering the freeway stretch. Equation (2.4) describes the boundary condition for vehicle speed at the outlet of the considered freeway stretch (i.e. at $\bar{x} = L$). This dynamic boundary condition reflects free-flow conditions at the downstream end, implying that even under congested situations, vehicles will still strive to reach the mixed speed, thereby achieving stable traffic flow; in other words, traffic flow at the right boundary is not obstructed. This boundary condition is realistic, as it does not require additional control measures, for example, keeping a constant density or speed at the outlet of the considered highway segment, while in practice it may appear in areas where at $\bar{x} = L$ there is an end of an area of low capacity (that calls for the implementation of control measures), such as, for example, the end of a tunnel or of a location of high curvature (see also Karafyllis *et al.* (2018)).

TABLE 1 *Description of traffic parameters involved in system (2.1)–(2.4) and (2.13)–(2.16)*

Parameters	Description in transportation system
$\rho_{\min} > 0$	The lowest value for density.
$L > 0$	The length of the highway segment under consideration.
$l > 0$	Average length of each vehicle.
$q_{\text{in}} > 0$	A constant external inflow.
$\tau_{\text{mix}} = \frac{1}{\frac{\alpha}{\tau_{\text{acc}}} + \frac{1-\alpha}{\tau_{\text{m}}}}$	The time constant of a mixture of ACC-equipped and human-driven vehicles.
$\tau_{\text{acc}} > 0$	The time constants of the ACC-equipped vehicles.
$\tau_{\text{m}} > 0$	The time constants of the manual vehicles.
$0 \leq \alpha \leq 1$	The proportion of ACC-equipped vehicles in the total vehicles.
$\bar{h}_{\text{acc}} > 0$	The steady-state time gap for ACC-equipped vehicles.
$\bar{h}_{\text{mix}} > 0$	The steady-state time gap for mixed vehicles.
$h_{\text{m}} > 0$	The time gap of manual vehicles.

The ARZ-type model can be interpreted both as a representation of traffic flow dynamics involving only manual vehicles (Zhang, 2002) and as a model describing traffic flow behaviour for situations where only ACC-equipped vehicles are present (Darbha & Rajagopal, 1999). Figure 1 shows a mixed traffic flow model representation with in-domain actuation using time-gap of ACC-equipped vehicles as a control. Note that in the mixed traffic case, to accommodate mixed traffic scenarios—where both ACC-equipped and manual vehicles coexist—we introduce the fundamental diagram relation for speed (Bekiaris-Liberis & Delis, 2021), expressed as

$$V_{\text{mix}}\left(\rho, h_{\text{acc}}\right) = \frac{1}{h_{\text{mix}}\left(h_{\text{acc}}\right)}\left(\frac{1}{\rho} - l\right), \tag{2.5}$$

where the effective (or mixed) time gap is defined as

$$h_{\text{mix}}\left(h_{\text{acc}}\right) = \frac{\alpha + (1-\alpha)\frac{\tau_{\text{acc}}}{\tau_{\text{m}}}}{\alpha + (1-\alpha)\frac{\tau_{\text{acc}}}{\tau_{\text{m}}}\frac{h_{\text{acc}}}{h_{\text{m}}}} h_{\text{acc}}, \tag{2.6}$$

where $\alpha \in [0, 1]$ denotes the proportion of ACC-equipped vehicles in the total vehicle population. This parameter governs the mixed traffic dynamics, as reflected in the speed equation above. In particular,

1. If only ACC-equipped vehicles exist, i.e. $\alpha = 1$, we have

$$V_{\text{acc}}\left(\rho, h_{\text{acc}}\right) = \frac{1}{h_{\text{acc}}}\left(\frac{1}{\rho} - l\right), \ \rho_{\min} < \rho < \frac{1}{l}. \tag{2.7}$$

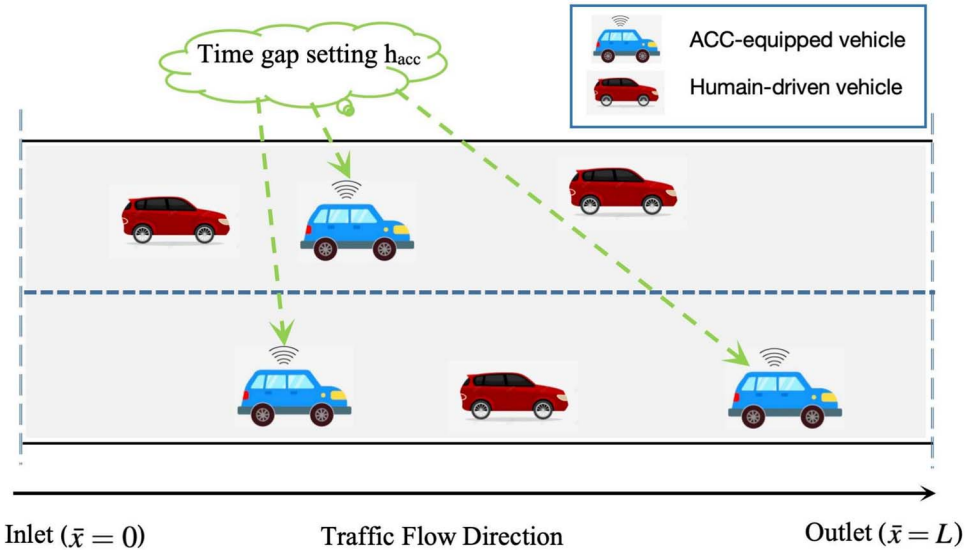

FIG. 1. Mixed traffic flow model representation with in-domain actuation using time-gap of ACC-equipped vehicles as a control (see also Manolis *et al.* (2020)).

2. If only manual vehicles are present, i.e. $\alpha = 0$, we have

$$V_{\mathrm{m}}(\rho) = \frac{1}{h_{\mathrm{m}}}\left(\frac{1}{\rho} - l\right), \ \rho_{\min} < \rho < \frac{1}{l}. \tag{2.8}$$

The formulations (2.7)–(2.8) correspond to the constant time-gap policy (in a direct correspondence to a microscopic viewpoint; refer to Darbha & Rajagopal (1999); Bose & Ioannou (2003) and Yi & Horowitz (2006) for more details).

To alleviate traffic congestion, the ARZ-type model (2.1)–(2.6) can be used for feedback-based control design. By dynamically adjusting the time gap $h_{\mathrm{acc}}(t, \bar{x})$ of ACC-equipped vehicles, traffic fluctuations can be mitigated, thereby ensuring more stable traffic flow.

2.2. *Linearization and diagonalization of the system*

The steady-state equilibria of system (2.1)–(2.4), resulting from a constant inflow rate q_{in} and a fixed, steady-state time gap for ACC-equipped vehicles, denoted by $\bar{h}_{\mathrm{acc}}$, lead to a steady-state mixed time gap expressed as

$$\bar{h}_{\mathrm{mix}} = \frac{\alpha + (1-\alpha)\frac{\tau_{\mathrm{acc}}}{\tau_{\mathrm{m}}}}{\alpha + (1-\alpha)\frac{\tau_{\mathrm{acc}}}{\tau_{\mathrm{m}}}\frac{\bar{h}_{\mathrm{acc}}}{h_{\mathrm{m}}}}\bar{h}_{\mathrm{acc}}. \tag{2.9}$$

The equilibria are uniform and fulfil the following condition:

$$\bar{v} = \frac{q_{\mathrm{in}}}{\bar{\rho}}, \tag{2.10}$$

where $\bar{\rho}$ and $\bar{v}$ represent, equilibrium, the constant traffic density and speed, respectively, achieved under a constant inflow q_{in} and a fixed time gap $\bar{h}_{\text{acc}}$, satisfying the following fundamental diagram relation (Bekiaris-Liberis & Delis, 2021, section 2-C):

$$\frac{1}{\bar{\rho}} - l = \bar{h}_{\text{mix}}\bar{v}, \tag{2.11}$$

where $1/\bar{\rho}$ represents the (equilibrium) average rear-to-rear distance between vehicles, which includes the length of the vehicle itself l and the bumper-to-bumper space gap between vehicles ($\bar{h}_{\text{mix}}\bar{v}$). It is worth noting that, to ensure consistency of units in (2.11), the term $1/\bar{\rho}$ should be interpreted as having distance units (e.g. [m] or [km]).

We define the error variables $\tilde{\rho}(t,\bar{x})$ and $\tilde{v}(t,\bar{x})$ as deviations of the traffic density $\rho(t,\bar{x})$ and traffic velocity $v(t,\bar{x})$ from their respective steady-state values $\bar{\rho}$ and $\bar{v}$. These are expressed as

$$\tilde{\rho}(t,\bar{x}) = \rho(t,\bar{x}) - \bar{\rho}, \quad \tilde{v}(t,\bar{x}) = v(t,\bar{x}) - \bar{v}. \tag{2.12}$$

Using (2.12), and linearizing the system (2.1)–(2.4) around the uniform, congested equilibrium profile, we get

$$\tilde{\rho}_t(t,\bar{x}) + \bar{v}\tilde{\rho}_{\bar{x}}(t,\bar{x}) = -\bar{\rho}\tilde{v}_{\bar{x}}(t,\bar{x}), \tag{2.13}$$

$$\tilde{v}_t(t,\bar{x}) - \frac{l}{\bar{h}_{\text{mix}}}\tilde{v}_{\bar{x}}(t,\bar{x}) = -\frac{1}{\bar{\rho}^2\tau_{\text{mix}}\bar{h}_{\text{mix}}}\tilde{\rho}(t,\bar{x}) - \frac{1}{\tau_{\text{mix}}}\tilde{v}(t,\bar{x}) - \frac{\alpha}{\tau_{\text{acc}}\bar{h}_{\text{acc}}^2}\left(\frac{1}{\bar{\rho}} - l\right)h_{\text{acc}}(t,\bar{x}), \tag{2.14}$$

$$\tilde{\rho}(t,0) = -\frac{\bar{\rho}}{\bar{v}}\tilde{v}(t,0), \tag{2.15}$$

$$\tilde{v}_t(t,L) = -\frac{1}{\bar{\rho}^2\tau_{\text{mix}}\bar{h}_{\text{mix}}}\tilde{\rho}(t,L) - \frac{1}{\tau_{\text{mix}}}\tilde{v}(t,L) - \frac{\alpha}{\tau_{\text{acc}}\bar{h}_{\text{acc}}^2}\left(\frac{1}{\bar{\rho}} - l\right)h_{\text{acc}}(t,L). \tag{2.16}$$

To simplify the analysis, namely the ISS stability analysis as conducted in Section 3, we introduce the following normalized spatial coordinate $x = \bar{x}/L$, where $x \in [0,1]$, which scales the highway segment of length L to a unit interval. This normalization, common in ISS analysis for PDEs (e.g. Karafyllis & Krstic (2018)), facilitates the stability analysis.

Introducing the following change of variables:

$$z(t,x) = \frac{\bar{v}}{\bar{\rho}}\left(\tilde{\rho}(t,Lx) + \frac{\bar{h}_{\text{mix}}\bar{\rho}}{(l+\bar{h}_{\text{mix}}\bar{v})}\tilde{v}(t,Lx)\right), \tag{2.17}$$

$$w(t,x) = \tilde{v}(t,Lx), \tag{2.18}$$

where $x \in [0,1]$, and using relation (2.11), we obtain the diagonal form of (2.13)–(2.16)

$$z_t(t,x) + \frac{\bar{v}}{L}z_x(t,x) = -\frac{1}{\tau_{\text{mix}}}z(t,x) - \bar{h}_{\text{mix}}\,\bar{\rho}\bar{v}\frac{\alpha}{\tau_{\text{acc}}\bar{h}_{\text{acc}}^2}\left(\frac{1}{\bar{\rho}} - l\right)U(t,x), \tag{2.19}$$

$$w_t(t,x) - \frac{l}{\bar{h}_{\text{mix}}L}w_x(t,x) = -\frac{1}{\bar{\rho}\bar{v}\tau_{\text{mix}}\bar{h}_{\text{mix}}}z(t,x) - \frac{\alpha}{\tau_{\text{acc}}\bar{h}_{\text{acc}}^2}\left(\frac{1}{\bar{\rho}} - l\right)U(t,x), \tag{2.20}$$

$$z(t,0) = -l\bar{\rho}w(t,0), \tag{2.21}$$

$$w_t(t,1) = -\frac{1}{\bar{\rho}\bar{v}\tau_{\text{mix}}\bar{h}_{\text{mix}}}z(t,1) - \frac{\alpha}{\tau_{\text{acc}}\bar{h}_{\text{acc}}^2}\left(\frac{1}{\bar{\rho}} - l\right)U(t,1), \tag{2.22}$$

with initial conditions

$$z(0,x) = \frac{\bar{v}}{\bar{\rho}}\left(\tilde{\rho}(0,Lx) + \frac{\bar{h}_{\text{mix}}\bar{\rho}}{(l+\bar{h}_{\text{mix}}\bar{v})}\tilde{v}(0,Lx)\right), \qquad w(0,x) = \tilde{v}_0(Lx), \tag{2.23}$$

and $U(t,x) = h_{acc}(t,Lx)$, $x \in [0,1]$. Note that although z incorporates information from both density and velocity, it is constructed via a scaling transformation and makes use of relation (2.11). Therefore, it has the same physical unit as w, i.e. metres per second ([m/s]).

2.3. *Feedback control law (nominal)*

We adapt the feedback control law proposed in (Bekiaris-Liberis & Delis, 2021, section III-B). We recall that such a control law stabilizes the traffic system exponentially by eliminating the source terms that cause the instability. The stability analysis is carried out in the $\mathscr{C}^1$-norm by means of Lyapunov techniques. In our study we use first the following nominal control (which differs from the one in Bekiaris-Liberis & Delis (2021) as we use a slightly different change of coordinates) to stabilize the system (2.19)–(2.22) exponentially

$$U(t,x) = \frac{\tau_{\text{acc}}\bar{h}_{\text{acc}}^2}{\alpha((1/\bar{\rho})-l)}\left(-\frac{1}{\bar{\rho}\bar{v}\tau_{\text{mix}}\bar{h}_{\text{mix}}}z(t,x) + \kappa w(t,x)\right), \tag{2.24}$$

with $\kappa > 0$. This feedback law aims at eliminating the source term in (2.20), which may cause instability due to a feedback connection between the states z and w.

2.4. *Emulation of the control law*

We aim at stabilizing system (2.19)–(2.22) on events while updating the nominal continuous-time controller $U(t,x)$ at certain sequence of time instants t_j, $j \in \mathbb{N}$, which will be characterized later on. The control value is held constant between two successive time instants and it is updated when some triggering conditions are verified. It is an efficient way to suitably apply (only when needed) the control value, thus avoiding useless actuation solicitations. To that end, we need to modify the control law. More precisely, the control law $U(t,x)$, which appears in (2.19)–(2.22) and is defined in (2.24), will be replaced by $U_d(t,x) = U(t_j,x)$ for all $x \in [0,1]$, and $t \in [t_j, t_{j+1})$, $j \geq 0$, that is,

$$U_d(t,x) = \frac{\tau_{\text{acc}}\bar{h}_{\text{acc}}^2}{\alpha((1/\bar{\rho})-l)}\left(-\frac{1}{\bar{\rho}\bar{v}\tau_{\text{mix}}\bar{h}_{\text{mix}}}z(t_j,x) + \kappa w(t_j,x)\right). \tag{2.25}$$

Hence, we deal with the following system with dynamic boundary condition:

$$z_t(t,x) + \frac{\bar{v}}{L}z_x(t,x) = -\frac{1}{\tau_{\text{mix}}}z(t,x) - \bar{h}_{\text{mix}}\,\bar{\rho}\bar{v}\frac{\alpha}{\tau_{\text{acc}}\bar{h}_{\text{acc}}^2}\left(\frac{1}{\bar{\rho}} - l\right)U_d(t,x), \tag{2.26}$$

$$w_t(t,x) - \frac{l}{\bar{h}_{\text{mix}}L}w_x(t,x) = -\frac{1}{\bar{\rho}\bar{v}\tau_{\text{mix}}\bar{h}_{\text{mix}}}z(t,x) - \frac{\alpha}{\tau_{\text{acc}}\bar{h}_{\text{acc}}^2}\left(\frac{1}{\bar{\rho}} - l\right)U_d(t,x), \tag{2.27}$$

$$z(t,0) = -l\bar{\rho}w(t,0), \tag{2.28}$$

$$w(t,1) = \eta(t), \tag{2.29}$$

$$\dot{\eta}(t) = -\frac{1}{\bar{\rho}\bar{v}\tau_{\text{mix}}\bar{h}_{\text{mix}}}z(t,1) - \frac{\alpha}{\tau_{\text{acc}}\bar{h}_{\text{acc}}^2}\left(\frac{1}{\bar{\rho}} - l\right)U_d(t,1), \tag{2.30}$$

for all $t \in [t_j, t_{j+1})$. We assume that the initial values satisfy the first-order compatibility conditions at the boundaries:

$$z_0(0) = -l\bar{\rho}\, w_0(0), \qquad w_0(1) = \eta(0), \tag{2.31}$$

so that we avoid introducing discontinuities or singularities at the boundaries.

Notice that $U_d(t,x) = U(t,x) + d^*(t,x)$, where $d^*(t,x)$ can be seen as an error of actuation (called deviation of actuation in the sequel of the paper). It is given as follows:

$$d^*(t,x) = \frac{\tau_{\text{acc}}\bar{h}_{\text{acc}}^2}{\alpha((1/\bar{\rho})-l)}\Big(-\frac{1}{\bar{\rho}\bar{v}\tau_{\text{mix}}\bar{h}_{\text{mix}}}\Big(z(t_j,x) - z(t,x)\Big) + \kappa\Big(w(t_j,x) - w(t,x)\Big)\Big), \tag{2.32}$$

for all $t \in [t_j, t_{j+1})$. Therefore, the closed-loop system, with dynamic boundary condition, reads as follows:

$$z_t(t,x) + \lambda_1 z_x(t,x) = -\kappa a w(t,x) - b_1 d^*(t,x), \tag{2.33}$$

$$w_t(t,x) - \lambda_2 w_x(t,x) = -\kappa w(t,x) - b_2 d^*(t,x), \tag{2.34}$$

$$z(t,0) = -r w(t,0), \tag{2.35}$$

$$w(t,1) = \eta(t), \tag{2.36}$$

$$\dot{\eta}(t) = -\kappa\eta(t) - b_2 d^*(t,1), \tag{2.37}$$

with

$$\begin{aligned}
\lambda_1 &:= \bar{v}L^{-1},\\
\lambda_2 &:= \tfrac{l}{\bar{h}_{\text{mix}}}L^{-1},\\
a &:= \bar{\rho}\bar{v}\bar{h}_{\text{mix}},\\
b_1 &:= \bar{h}_{\text{mix}}\,\bar{\rho}\bar{v}\tfrac{\alpha}{\tau_{\text{acc}}\bar{h}_{\text{acc}}^2}\Big(\tfrac{1}{\bar{\rho}} - l\Big),\\
b_2 &:= \tfrac{\alpha}{\tau_{\text{acc}}\bar{h}_{\text{acc}}^2}\Big(\tfrac{1}{\bar{\rho}} - l\Big),\\
r &:= l\bar{\rho}.
\end{aligned} \tag{2.38}$$

3. ETC strategy and main results

In this section, we introduce the ETC and the main results: the well-posedness of the closed-loop system under an ETC, the existence of a lower bound to the time interval between two consecutive switches and the exponential stability of the closed-loop system under the ETC. By building on the emulation approach, we define first the ETC considered in this paper. It encloses both a triggering condition (which determines the time instant at which the controller needs to be updated) and the feedback control (2.25). The proposed event-triggering condition is based on the evolution of sup-norm of the actuation deviation (2.32) and the evolution of the sup-norm of the states.

DEFINITION 1. Let $\beta_1, \beta_2 > 0$ be design parameters. The ETC is defined by considering the following components:

(I) (The event-triggered mechanism) The times of the events $t_j \geq 0$ with $t_0 = 0$ form a finite or countable set of times, which is determined by the following rules for some $j \geq 0$:

(a) if $\left\{t \in \mathbb{R}_+ | t > t_j \wedge \|d^*(t,\cdot)\|_\infty \geq \beta_1 \|z(t,\cdot)\|_\infty + \beta_2 \|w(t,\cdot)\|_\infty\right\} = \emptyset$ then the set of the times of the events is $\{t_0, ..., t_j\}$,

(b) if $\left\{t \in \mathbb{R}_+ | t > t_j \wedge \|d^*(t,\cdot)\|_\infty \geq \beta_1 \|z(t,\cdot)\|_\infty + \beta_2 \|w(t,\cdot)\|_\infty\right\} \neq \emptyset$ then the next event time is given by

$$t_{j+1} = \inf\left\{t \in \mathbb{R}_+ | t > t_j \wedge \|d^*(t,\cdot)\|_\infty \geq \beta_1 \|z(t,\cdot)\|_\infty + \beta_2 \|w(t,\cdot)\|_\infty\right\}, \tag{3.1}$$

where the actuation deviation $d^*(t,x)$ is given by (2.32) for all $t \in [t_j, t_{j+1})$.

(II) (The control action) The feedback control law is defined by (2.25) for all $t \in [t_j, t_{j+1})$.

3.1. *Well-posedness aspects*

PROPOSITION 1. For any given initial data $\big(z(t_j,x), w(t_j,x)\big) \in (L^\infty(0,1))^2$, there exists a unique solution $\big(z,w\big) \in \mathscr{C}^0\big([t_j, t_{j+1}]; (L^\infty(0,1))^2\big)$ to the system (2.33)–(2.37).

Proof. The boundary input (2.37) is given by an absolutely continuous ODE solution and the in-domain source terms are reset to zero at each triggering instant, for all $x \in [0,1]$. Inspired by Prieur *et al.* (2014)—where the hyperbolic PDE is affected by source terms that are subject to switching—we adopt the notion of solution along the characteristics for all $t \in [t_j, t_{j+1})$. Hence, we have that for $t_j \leq t \leq t_j + \frac{x}{\lambda_1}$, the solution $z(t,x)$ is given as

$$z(t,x) = z\left(t_j, x - \lambda_1(t - t_j)\right) + \int_{t_j}^{t} (-\kappa a) w(\tau, x - \lambda_1(t-\tau))d\tau + \int_{t_j}^{t} (-b_1) d^*(\tau, x - \lambda_1(t-\tau))d\tau. \tag{3.2}$$

For $t_j + \frac{x}{\lambda_1} \leq t < t_{j+1}$, it is expressed as

$$z(t,x) = -rw\left(t - \tfrac{x}{\lambda_1}, 0\right) + \int_{t-\frac{x}{\lambda_1}}^{t} (-\kappa a) w(\tau, x - \lambda_1(t-\tau))d\tau + \int_{t-\frac{x}{\lambda_1}}^{t} (-b_1) d^*(\tau, x - \lambda_1(t-\tau))d\tau. \tag{3.3}$$

For $t_j \leq t \leq t_j + \frac{1-x}{\lambda_2}$, the solution $w(t,x)$ satisfies

$$w(t,x) = w\left(t_j, x + \lambda_2(t - t_j)\right) \exp(-\kappa(t-t_j)) + \int_{t_j}^{t} \exp(-\kappa(t-\tau))(-b_2) d^*(\tau, x + \lambda_2(t-\tau))d\tau. \tag{3.4}$$

For $t_j + \frac{1-x}{\lambda_2} \le t < t_{j+1}$, it is given as

$$w(t,x) = \eta\left(t - \tfrac{1-x}{\lambda_2}\right)\exp\left(-\tfrac{\kappa}{\lambda_2}(1-x)\right) + \int_{t-\frac{1-x}{\lambda_2}}^{t} \exp(-\kappa(t-\tau))(-b_2)d^*(\tau, x+\lambda_2(t-\tau))d\tau, \tag{3.5}$$

where $\eta(t)$ evolves as

$$\eta(t) = \exp(-\kappa(t-t_j))\eta(t_j) - b_2\int_{t_j}^{t}\exp(-\kappa(t-\tau))d^*(\tau,1)\,d\tau. \tag{3.6}$$

The characteristic-based explicit solution guarantees the existence and uniqueness of a solution $\left(z,w\right) \in \mathscr{C}^0\left([t_j,t_{j+1}];(L^\infty(0,1))^2\right)$ over the time interval $[t_j,t_{j+1}]$. □

The methodology of Prieur *et al.* (2014) is adapted to account for the ODE-driven boundary condition (2.37), which gives rise to a solution that is absolutely continuous. Since our analysis guarantees existence and uniqueness of a solution in $\mathscr{C}^0([t_j,t_{j+1}];(L^\infty(0,1))^2)$ for each interval $[t_j,t_{j+1}]$, we view such a solution as weak. To extend the solution on $[0,\lim_{j\to\infty} t_j)$, one can employ a step-by-step method using Proposition 1, iterating over successive intervals $[t_j,t_{j+1}]$. To ensure the solution is well-posed for all $t \ge 0$, it is essential to verify that the triggering times satisfy $\lim_{j\to\infty} t_j = +\infty$.

3.2. *Stability analysis*

In this section, we provide the stability properties of the closed-loop system (2.33)–(2.37). In the following Lemma 1, we first state the estimates of the ISS stability of the closed-loop system, which is essential for the stability analysis of system (2.33)–(2.37).

LEMMA 1. Consider the closed-loop system (2.33)–(2.37) with initial data $z(0,x) = z_0$ and $w(0,x) = w_0$ where $(z_0,w_0) \in (L^\infty(0,1))^2$. The following estimates hold, for some $\varsigma \in (0,\kappa)$, and for all $t \in [0,\lim_{j\to\infty}(t_j))$:

$$\begin{aligned}\|z(t,\cdot)\|_\infty \le{}& e^{-\varsigma t}e^{\frac{\varsigma}{\lambda_1}}\|z(0,\cdot)\|_\infty \\ &+ \tfrac{2|b_1|}{\lambda_1}e^{\left(\frac{|\kappa a|+|b_1|}{|b_1|}+\frac{\varsigma}{\lambda_1}\right)}\max_{\max\left\{0,t-\frac{1}{\lambda_1}\right\}\le s\le t}\left(\left(\|d^*(s,\cdot)\|_\infty + \|w(s,\cdot)\|_\infty\right)e^{-\varsigma(t-s)}\right) \\ &+ e^{\frac{\varsigma}{\lambda_1}}|r|\max_{\max\left\{0,t-\frac{1}{\lambda_1}\right\}\le s\le t}\left(|w(s,0)|e^{-\varsigma(t-s)}\right),\end{aligned} \tag{3.7}$$

$$\begin{aligned}\|w(t,\cdot)\|_\infty \le{}& e^{-\varsigma t}e^{\frac{\varsigma}{\lambda_2}}\|w(0,\cdot)\|_\infty + \tfrac{|b_2|}{\lambda_2}e^{\left(1-\frac{\kappa}{\lambda_2}+\frac{\varsigma}{\lambda_2}\right)}\max_{\max\left\{0,t-\frac{1}{\lambda_2}\right\}\le s\le t}\left(\|d^*(s,\cdot)\|_\infty e^{-\varsigma(t-s)}\right) \\ &+ e^{\frac{\varsigma}{\lambda_2}}\max_{\max\left\{0,t-\frac{1}{\lambda_2}\right\}\le s\le t}\left(|\eta(s)|e^{-\varsigma(t-s)}\right)\end{aligned} \tag{3.8}$$

and

$$|\eta(t)| \leq e^{-\varsigma t}|\eta(0)| + \tfrac{|b_2|}{\kappa-\varsigma} \max_{0\leq s\leq t}\left(|d^*(s,1)|e^{-\varsigma(t-s)}\right). \tag{3.9}$$

Proof. See the appendix. □

Let us first state the following small-gain condition, which indicates the choice of β_1, β_2 (the parameters involved in the triggering condition (3.1)):

$$\begin{aligned}&\beta_1\left(\tfrac{|b_2||r|}{\kappa} + \tfrac{|r||b_2|}{\lambda_2}e^{\left(1-\frac{\kappa}{\lambda_2}\right)} + \tfrac{2|b_1b_2|}{\lambda_1\lambda_2}e^{\left(\frac{|\kappa a|+|b_1|}{|b_1|}\right)}e^{\left(1-\frac{\kappa}{\lambda_2}\right)} + \tfrac{2|b_1|}{\lambda_1}e^{\left(\frac{|\kappa a|+|b_1|}{|b_1|}\right)}\tfrac{|b_2|}{\kappa} + \tfrac{2|b_1|}{\lambda_1}e^{\left(\frac{|\kappa a|+|b_1|}{|b_1|}\right)}\right)\\ &+\beta_2\left(\tfrac{|b_2|}{\lambda_2}e^{\left(1-\frac{\kappa}{\lambda_2}\right)} + \tfrac{|b_2|}{\kappa}\right) < 1.\end{aligned} \tag{3.10}$$

By continuity arguments, there exists $\varsigma > 0$ sufficiently small, and $\varsigma < \kappa$, such that

$$\begin{aligned}&\beta_1\Lambda^2(\varsigma)\left(\tfrac{|b_2||r|}{\kappa-\varsigma} + \tfrac{|r||b_2|}{\lambda_2}e^{\left(1-\frac{\kappa}{\lambda_2}\right)}\right) + \beta_1\Lambda^2(\varsigma)\tfrac{2|b_1|}{\lambda_1}e^{\left(\frac{|\kappa a|+|b_1|}{|b_1|}\right)}\left(\tfrac{|b_2|}{\lambda_2}e^{\left(1-\frac{\kappa}{\lambda_2}\right)} + \tfrac{|b_2|}{\kappa-\varsigma}\right)\\ &+\beta_1\Lambda(\varsigma)\tfrac{2|b_1|}{\lambda_1}e^{\left(\frac{|\kappa a|+|b_1|}{|b_1|}\right)} + \beta_2\Lambda(\varsigma)\left(\tfrac{|b_2|}{\lambda_2}e^{\left(1-\frac{\kappa}{\lambda_2}\right)} + \tfrac{|b_2|}{\kappa-\varsigma}\right) < 1,\end{aligned} \tag{3.11}$$

where

$$\Lambda(\varsigma) = e^{\varsigma\left(\frac{1}{\lambda_1}+\frac{1}{\lambda_2}\right)}. \tag{3.12}$$

The existence of ς is assured because the function

$$\begin{aligned}\mathscr{F}(\varsigma) =&\beta_1\Lambda^2(\varsigma)\left(\tfrac{|b_2||r|}{\kappa-\varsigma} + \tfrac{|r||b_2|}{\lambda_2}e^{\left(1-\frac{\kappa}{\lambda_2}\right)}\right) + \beta_1\Lambda^2(\varsigma)\tfrac{2|b_1|}{\lambda_1}e^{\left(\frac{|\kappa a|+|b_1|}{|b_1|}\right)}\left(\tfrac{|b_2|}{\lambda_2}e^{\left(1-\frac{\kappa}{\lambda_2}\right)}\tfrac{|b_2|}{\kappa-\varsigma}\right)\\ &+\beta_1\Lambda(\varsigma)\tfrac{2|b_1|}{\lambda_1}e^{\left(\frac{|\kappa a|+|b_1|}{|b_1|}\right)} + \beta_2\Lambda(\varsigma)\left(\tfrac{|b_2|}{\lambda_2}e^{\left(1-\frac{\kappa}{\lambda_2}\right)} + \tfrac{|b_2|}{\kappa-\varsigma}\right),\end{aligned}$$

is continuous at 0 and satisfies $\mathscr{F}(0) < 1$. Furthermore, it also holds that $0 < \beta_1\Lambda(\varsigma)\frac{2|b_1|}{\lambda_1}e^{\left(\frac{|\kappa a|+|b_1|}{|b_1|}\right)} < 1$, and $0 < \beta_2\Lambda(\varsigma)\left(\frac{|b_2|}{\lambda_2}e^{\left(1-\frac{\kappa}{\lambda_2}\right)} + \frac{|b_2|}{\kappa-\varsigma}\right) < 1$. Reorganizing the terms, we introduce the following quantities as defined from (3.11):

$$\phi_1 := \tfrac{2|b_1|}{\lambda_1}e^{\left(\frac{|\kappa a|+|b_1|}{|b_1|}\right)}, \tag{3.13}$$

$$\phi_2 := \tfrac{|b_2|}{\lambda_2}e^{\left(1-\frac{\kappa}{\lambda_2}\right)} \tag{3.14}$$

and

$$\phi_3(\varsigma) := \tfrac{|b_2|}{\kappa-\varsigma}. \tag{3.15}$$

Additionally, we define

$$\Phi := \beta_1 \Lambda(\varsigma)^2 \left(1-\beta_1\Lambda(\varsigma)\phi_1\right)^{-1} (1-\beta_2\Lambda(\varsigma)(\phi_2+\phi_3(\varsigma)))^{-1}(\phi_2+\phi_3(\varsigma))(|r|+\beta_2\phi_1+\phi_1). \tag{3.16}$$

We can ensure that if (3.11) is verified, then $\Phi < 1$. This condition is instrumental in the proof of the main result that we state next.

THEOREM 1. Assume $\beta_1, \beta_2 > 0$ are chosen such that the condition (3.10) is satisfied. Then, for any initial conditions $(z_0, w_0) \in (L^\infty(0,1))^2$ and $\eta(0) \in \mathbb{R}$ satisfying the compatibility condition (2.31), there exist constants $\varsigma > 0$ and $\Theta > 0$ such that the following estimates hold for the solutions to the closed-loop system (2.26)–(2.30) with the ETC law (2.25), (3.1):

$$\|z(t,\cdot)\|_\infty + \|w(t,\cdot)\|_\infty + |\eta(t)| \le \Theta \exp(-\varsigma t)\Big(\|z_0\|_\infty + \|w_0\|_\infty + |\eta(0)|\Big), \tag{3.17}$$

for all $t \in [0, \lim_{j\to\infty}(t_j))$.

Proof. : According to Lemma 1, the ISS bounds provided in (3.7)–(3.9) lead to the following alternative, yet more conservative, estimates, for all $t \in [0, \lim_{j\to\infty}(t_j))$:

$$\begin{aligned}\|z(t,\cdot)\|_\infty &\le e^{-\varsigma t} e^{\frac{\varsigma}{\lambda_1}} \|z(0,\cdot)\|_\infty + \phi_1\Lambda(\varsigma) \max_{0\le s\le t}\left(\left(\|d^*(s,\cdot)\|_\infty + \|w(s,\cdot)\|_\infty\right) e^{-\varsigma(t-s)}\right) \\ &\quad + \Lambda(\varsigma)|r| \max_{0\le s\le t}\left(\|w(s,\cdot)\|_\infty e^{-\varsigma(t-s)}\right), \end{aligned} \tag{3.19}$$

$$\begin{aligned}\|w(t,\cdot)\|_\infty &\le e^{-\varsigma t} e^{\frac{\varsigma}{\lambda_2}} \|w(0,\cdot)\|_\infty + \phi_2\Lambda(\varsigma) \max_{0\le s\le t}\left(\|d^*(s,\cdot)\|_\infty e^{-\varsigma(t-s)}\right) \\ &\quad + \Lambda(\varsigma) \max_{0\le s\le t}\left(|\eta(s)| e^{-\varsigma(t-s)}\right) \end{aligned} \tag{3.19}$$

and

$$|\eta(t)| \le e^{-\varsigma t}|\eta(0)| + \phi_3(\varsigma) \max_{0\le s\le t}\left(|d^*(s,1)| e^{-\varsigma(t-s)}\right), \tag{3.20}$$

where $\Lambda(\varsigma)$ is defined in (3.12), while ϕ_1, ϕ_2 and $\phi_3(\varsigma)$ are defined in (3.13), (3.14) and (3.15), respectively. Additionally, we define the following quantities for all $t \in [0, \lim_{j\to\infty}(t_j))$ and $x \in [0,1]$:

$$\begin{aligned}
\|z\|_{[0,t]} &:= \max_{0\le s\le t} \left(\|z(s,\cdot)\|_\infty e^{\varsigma s}\right),\\
\|w\|_{[0,t]} &:= \max_{0\le s\le t} \left(\|w(s,\cdot)\|_\infty e^{\varsigma s}\right),\\
\|\eta\|_{[0,t]} &:= \max_{0\le s\le t} \left(|\eta(s)| e^{\varsigma s}\right),\\
\left\|d^*\right\|_{[0,t]} &:= \max_{0\le s\le t} \left(\left\|d^*(s,\cdot)\right\|_\infty e^{\varsigma s}\right).
\end{aligned} \tag{3.21}$$

Using the relations (3.18)–(3.20) together with (3.21), we derive

$$\|z\|_{[0,t]} \le e^{\frac{\varsigma}{\lambda_1}} \left\|z_0\right\|_\infty + \Lambda(\varsigma)|r|\, \|w\|_{[0,t]} + \phi_1 \Lambda(\varsigma) \left(\|d^*\|_{[0,t]} + \|w\|_{[0,t]}\right), \tag{3.22}$$

$$\|w\|_{[0,t]} \le e^{\frac{\varsigma}{\lambda_2}} \left\|w_0\right\|_\infty + \Lambda(\varsigma)\, \|\eta\|_{[0,t]} + \phi_2 \Lambda(\varsigma) \left\|d^*\right\|_{[0,t]} \tag{3.23}$$

and

$$\|\eta\|_{[0,t]} \le |\eta(0)| + \phi_3(\varsigma) \left\|d^*\right\|_{[0,t]}. \tag{3.24}$$

From Definition 1, events are triggered to guarantee, for all $t \in [0, \lim_{j\to\infty}(t_j))$,

$$\|d^*(t,\cdot)\|_\infty \le \beta_1 \|z(t,\cdot)\|_\infty + \beta_2 \|w(t,\cdot)\|_\infty. \tag{3.25}$$

Therefore, from (3.22)–(3.24) along with definitions (3.21), it follows that

$$\|z\|_{[0,t]} \le e^{\frac{\varsigma}{\lambda_1}} \left\|z_0\right\|_\infty + (\Lambda(\varsigma)|r| + \beta_2 \Lambda(\varsigma)\phi_1 + \Lambda(\varsigma)\phi_1)\, \|w\|_{[0,t]} + \beta_1 \Lambda(\varsigma)\phi_1 \|z\|_{[0,t]}, \tag{3.26}$$

$$\|w\|_{[0,t]} \le e^{\frac{\varsigma}{\lambda_2}} \left\|w_0\right\|_\infty + \Lambda(\varsigma)\, \|\eta\|_{[0,t]} + \beta_1 \Lambda(\varsigma)\phi_2 \|z\|_{[0,t]} + \beta_2 \Lambda(\varsigma)\phi_2 \|w\|_{[0,t]} \tag{3.27}$$

and

$$\|\eta\|_{[0,t]} \le |\eta(0)| + \beta_1 \phi_3(\varsigma) \|z\|_{[0,t]} + \beta_2 \phi_3(\varsigma) \|w\|_{[0,t]}. \tag{3.28}$$

Replacing (3.28) with (3.27), we get

$$\begin{aligned}
\|w\|_{[0,t]} &\le e^{\frac{\varsigma}{\lambda_2}} \left\|w_0\right\|_\infty + \Lambda(\varsigma)|\eta_0| + \Lambda(\varsigma)\beta_1\phi_3(\varsigma)\|z\|_{[0,t]} + \Lambda(\varsigma)\beta_2\phi_3(\varsigma)\|w\|_{[0,t]}\\
&\quad + \beta_1 \Lambda(\varsigma)\phi_2 \|z\|_{[0,t]} + \beta_2 \Lambda(\varsigma)\phi_2 \|w\|_{[0,t]}\\
&\le e^{\frac{\varsigma}{\lambda_2}} \left\|w_0\right\|_\infty + \Lambda(\varsigma)|\eta_0| + \beta_1 \Lambda(\varsigma) \left(\phi_3(\varsigma) + \phi_2\right) \|z\|_{[0,t]} + \beta_2 \Lambda(\varsigma) \left(\phi_3(\varsigma) + \phi_2\right) \|w\|_{[0,t]}.
\end{aligned}$$

Therefore, it holds

$$\begin{aligned}\|z\|_{[0,t]} \leq\ & \left(1-\beta_1\Lambda(\varsigma)\phi_1\right)^{-1} e^{\frac{\varsigma}{\lambda_1}} \left\|z_0\right\|_\infty + \left(1-\beta_1\Lambda(\varsigma)\phi_1\right)^{-1} (\Lambda(\varsigma)|r| \\ & + \beta_2\Lambda(\varsigma)\phi_1 + \Lambda(\varsigma)\phi_1) \|w\|_{[0,t]}\,, \end{aligned} \tag{3.29}$$

and

$$\begin{aligned}\|w\|_{[0,t]} \leq\ & (1-\beta_2\Lambda(\varsigma)\psi_{2,3}(\varsigma))^{-1} e^{\frac{\varsigma}{\lambda_2}} \left\|w_0\right\|_\infty + (1-\beta_2\Lambda(\varsigma)\psi_{2,3}(\varsigma))^{-1}\Lambda(\varsigma)|\eta_0| \\ & + (1-\beta_2\Lambda(\varsigma)\psi_{2,3}(\varsigma))^{-1}\beta_1\Lambda(\varsigma)\psi_{2,3}(\varsigma)\|z\|_{[0,t]}, \end{aligned} \tag{3.30}$$

with

$$\psi_{2,3}(\varsigma) := \phi_2 + \phi_3(\varsigma). \tag{3.31}$$

By substituting (3.30) into (3.29), we obtain

$$\begin{aligned}\|z\|_{[0,t]} \leq\ & \left(1-\beta_1\Lambda(\varsigma)\phi_1\right)^{-1} e^{\frac{\varsigma}{\lambda_1}} \left\|z_0\right\|_\infty \\ & + \left(1-\beta_1\Lambda(\varsigma)\phi_1\right)^{-1} (\Lambda(\varsigma)|r| + \beta_2\Lambda(\varsigma)\phi_1 + \Lambda(\varsigma)\phi_1)(1-\beta_2\Lambda(\varsigma)\psi_{2,3}(\varsigma))^{-1} e^{\frac{\varsigma}{\lambda_2}} \left\|w_0\right\|_\infty \\ & + \left(1-\beta_1\Lambda(\varsigma)\phi_1\right)^{-1} (\Lambda(\varsigma)|r| + \beta_2\Lambda(\varsigma)\phi_1 + \Lambda(\varsigma)\phi_1)(1-\beta_2\Lambda(\varsigma)\psi_{2,3}(\varsigma))^{-1}\Lambda(\varsigma)|\eta_0| \\ & + \beta_1\Lambda(\varsigma)\left(1-\beta_1\Lambda(\varsigma)\phi_1\right)^{-1} (1-\beta_2\Lambda(\varsigma)\psi_{2,3}(\varsigma))^{-1}\psi_{2,3}(\varsigma)(\Lambda(\varsigma)|r| \\ & + \beta_2\Lambda(\varsigma)\phi_1 + \Lambda(\varsigma)\phi_1)\|z\|_{[0,t]}. \end{aligned} \tag{3.32}$$

Replacing (3.29) with (3.30), we get

$$\begin{aligned}\|w\|_{[0,t]} \leq & (1-\beta_2\Lambda(\varsigma)\psi_{2,3}(\varsigma))^{-1} e^{\frac{\varsigma}{\lambda_2}} \left\|w_0\right\|_\infty + (1-\beta_2\Lambda(\varsigma)\psi_{2,3}(\varsigma))^{-1}\Lambda(\varsigma)|\eta_0| \\ & + (1-\beta_2\Lambda(\varsigma)\psi_{2,3}(\varsigma))^{-1}\beta_1\Lambda(\varsigma)\psi_{2,3}(\varsigma)\left(1-\beta_1\Lambda(\varsigma)\phi_1\right)^{-1} e^{\frac{\varsigma}{\lambda_1}} \left\|z_0\right\|_\infty \\ & + \beta_1\left(1-\beta_1\Lambda(\varsigma)\phi_1\right)^{-1} (1-\beta_2\Lambda(\varsigma)\psi_{2,3}(\varsigma))^{-1}\Lambda(\varsigma)\psi_{2,3}(\varsigma)(\Lambda(\varsigma)|r| \\ & + \beta_2\Lambda(\varsigma)\phi_1 + \Lambda(\varsigma)\phi_1)\|w\|_{[0,t]}\,. \end{aligned} \tag{3.33}$$

Hence, we can finally obtain

$$\begin{aligned}\|z\|_{[0,t]} \leq & (1-\Phi)^{-1}\left(1-\beta_1\Lambda(\varsigma)\phi_1\right)^{-1}\Lambda(\varsigma)\left\|z_0\right\|_\infty \\ & + (1-\Phi)^{-1}\left(1-\beta_1\Lambda(\varsigma)\phi_1\right)^{-1}(\Lambda(\varsigma)|r| + \beta_2\Lambda(\varsigma)\phi_1 + \Lambda(\varsigma)\phi_1) \\ & \times (1-\beta_2\Lambda(\varsigma)\psi_{2,3}(\varsigma))^{-1}\Lambda(\varsigma)\left\|w_0\right\|_\infty \\ & + (1-\Phi)^{-1}\left(1-\beta_1\Lambda(\varsigma)\phi_1\right)^{-1}(\Lambda(\varsigma)|r| + \beta_2\Lambda(\varsigma)\phi_1 + \Lambda(\varsigma)\phi_1) \\ & \times (1-\beta_2\Lambda(\varsigma)\psi_{2,3}(\varsigma))^{-1}\Lambda(\varsigma)|\eta_0|, \end{aligned} \tag{3.34}$$

and

$$\begin{aligned}\|w\|_{[0,t]} \leq\ & (1-\Phi)^{-1}\left(1-\beta_2\Lambda(\varsigma)\psi_{2,3}(\varsigma)\right)^{-1}\Lambda(\varsigma)\left\|w_0\right\|_\infty \\ & + (1-\Phi)^{-1}\left(1-\beta_2\Lambda(\varsigma)\psi_{2,3}(\varsigma)\right)^{-1}\Lambda(\varsigma)|\eta_0| \\ & + (1-\Phi)^{-1}\left(1-\beta_2\Lambda(\varsigma)\psi_{2,3}(\varsigma)\right)^{-1}\beta_1\Lambda(\varsigma)\psi_{2,3}(\varsigma)\left(1-\beta_1\Lambda(\varsigma)\phi_1\right)^{-1}\Lambda(\varsigma)\left\|z_0\right\|_\infty,\end{aligned} \tag{3.35}$$

where Φ is given by

$$\Phi = \beta_1\Lambda(\varsigma)^2\left(1-\beta_1\Lambda(\varsigma)\phi_1\right)^{-1}\left(1-\beta_2\Lambda(\varsigma)\psi_{2,3}(\varsigma)\right)^{-1}\psi_{2,3}(\varsigma)(|r|+\beta_2\phi_1+\phi_1), \tag{3.36}$$

which is precisely defined in (3.16). It satisfies $\Phi < 1$ due to the validity of (3.11). Combining (3.34), (3.35) and (3.28), we can infer that (3.17) is true for a suitable constant Θ, for all $t \in [0, \lim_{j\to\infty}(t_j))$. Thus, the proof is concluded. □

REMARK 1. The convergence speed, determined by the decay rate ς, is influenced by the feedback gain κ and triggering parameters β_1 and β_2. Larger κ enhances convergence but may increase the number of events due to tighter triggering thresholds (smaller β_1, β_2), as the small-gain condition (3.10) balances stability and actuation frequency.

3.3. *Avoidance of the Zeno phenomenon and exponential stability result*

THEOREM 2. Under the event-triggered condition (3.1), any inter-sampling interval is lower bounded by a positive constant (depending on the current state at t_j).

Proof. : Notice that if the set of triggering times is empty, then the next event is not triggered. Moreover, the estimates in Theorem 1 guarantee that for $t > t_j$ if $\|z(t_j,\cdot)\|_\infty = \|w(t_j,\cdot)\|_\infty \equiv 0$, then $\|z(t,\cdot)\|_\infty = \|w(t,\cdot)\|_\infty \equiv 0$. Since zero states at t_j indicate that the system has achieved equilibrium in finite time, the triggering mechanism will not activate further events, and the system remains in its zero equilibrium. In another case, assume that $\|z(t_j,\cdot)\|_\infty = \|w(t_j,\cdot)\|_\infty \equiv 0$, but there exists a $t > t_j$ such that either $\|z(t,\cdot)\|_\infty > 0$ or $\|w(t,\cdot)\|_\infty > 0$. This would mean the system deviates from the equilibrium after t_j, which contradicts the system's dynamics and estimates in Theorem 1. In these cases, $t_{j+1} = +\infty$, and thus the Zeno phenomenon is excluded. Assume that we do not have those cases. From the definition of the deviation of actuation (2.32), the following estimate holds:

$$\|d^*(t,\cdot)\|_\infty \ \leq\ R\Big(\|z(t_j,\cdot)-z(t,\cdot)\|_\infty + \|w(t_j,\cdot)-w(t,\cdot)\|_\infty\Big), \tag{3.37}$$

where

$$R := \max\left(\left|\frac{\tau_{\text{acc}}\bar{h}_{\text{acc}}^2}{\alpha((1/\bar{\rho})-l)}\frac{1}{\bar{\rho}\tau_{\text{mix}}\bar{h}_{\text{mix}}}\right|, \left|\frac{\tau_{\text{acc}}\bar{h}_{\text{acc}}^2}{\alpha((1/\bar{\rho})-l)}\kappa\right|\right). \tag{3.38}$$

Consider the following inequality:

$$\|z(t_j,\cdot)-z(t,\cdot)\|_\infty+\|w(t_j,\cdot)-w(t,\cdot)\|_\infty\leq\tfrac{\beta_1}{R}\|z(t,\cdot)\|_\infty+\tfrac{\beta_2}{R}\|w(t,\cdot)\|_\infty. \tag{3.39}$$

Notice that by enforcing (3.39) we guarantee $\|d^*(t,\cdot)\|_\infty\leq\beta_1\|z(t,\cdot)\|_\infty+\beta_2\|w(t,\cdot)\|_\infty$, which is the triggering condition in (3.1) under which Theorem 1 applies. Moreover, consider the following more conservative inequality:

$$\|z(t_j,\cdot)-z(t,\cdot)\|_\infty+\|w(t_j,\cdot)-w(t,\cdot)\|_\infty\leq\tfrac{\beta_1}{R+\beta_1}\|z(t_j,\cdot)\|_\infty+\tfrac{\beta_2}{R+\beta_2}\|w(t_j,\cdot)\|_\infty. \tag{3.40}$$

It can be proved (using the property in (Liu *et al.*, 2020, lemma B3)) that if (3.40) is verified then (3.39) holds. Therefore, by enforcing (3.40) we guarantee $\|d^*(t,\cdot)\|_\infty\leq\beta_1\|z(t,\cdot)\|_\infty+\beta_2\|w(t,\cdot)\|_\infty$, as well. It suffices then to show the inter-executions times are bounded for the execution rule $\|z(t_j,\cdot)-z(t,\cdot)\|_\infty+\|w(t_j,\cdot)-w(t,\cdot)\|_\infty\geq\frac{\beta_1}{R+\beta_1}\|z(t_j,\cdot)\|_\infty+\frac{\beta_2}{R+\beta_2}\|w(t_j,\cdot)\|_\infty$. Based on this condition, we define the function

$$\psi(t):=\frac{\|z(t_j,\cdot)-z(t,\cdot)\|_\infty+\|w(t_j,\cdot)-w(t,\cdot)\|_\infty}{\frac{\beta_1}{R+\beta_1}\|z(t_j,\cdot)\|_\infty+\frac{\beta_2}{R+\beta_2}\|w(t_j,\cdot)\|_\infty}. \tag{3.41}$$

A lower bound for the inter-execution times is given by the time that takes for the function ψ to go from $\psi(t_j)=0$ to $\psi(t_{j+1}^-)=1$ (here t_{j+1}^- is the left limit at $t=t_{j+1}$). The time-derivative of ψ on (t_j,t_{j+1}) can be computed by adapting the arguments in (Karafyllis & Krstic, 2021, lemma 5.2) to our case, and considering the following:

$$\tfrac{d\|z(t_j,\cdot)-z(t,\cdot)\|_\infty}{dt}\leq\|\tfrac{\partial}{\partial t}(z(t_j,x)-z(t,x))\|_\infty, \tag{3.42}$$

$$\tfrac{d\|w(t_j,\cdot)-w(t,\cdot)\|_\infty}{dt}\leq\|\tfrac{\partial}{\partial t}(w(t_j,x)-w(t,x))\|_\infty. \tag{3.43}$$

If $\|z(t_j,\cdot)-z(t,\cdot)\|_\infty>0$ and $\|w(t_j,\cdot)-w(t,\cdot)\|_\infty>0$, for $t\in(t_j,t_{j+1})$, using (3.42) and (3.43), we have

$$\tfrac{d\|z(t_j,\cdot)-z(t,\cdot)\|_\infty}{dt}\leq\max_{x\in I(t)}\Big(sgn(z(t_j,x)-z(t,x))(\tfrac{\partial}{\partial t}(z(t_j,x)-z(t,x)))\Big), \tag{3.44}$$

$$\tfrac{d\|w(t_j,\cdot)-w(t,\cdot)\|_\infty}{dt}\leq\max_{x\in I(t)}\Big(sgn(w(t_j,x)-w(t,x))(\tfrac{\partial}{\partial t}(w(t_j,x)-w(t,x)))\Big), \tag{3.45}$$

$I(t)=\{x\in[0,1]:|y(t,x)|=\|y(t,\cdot)\|_\infty\}$. Here, y may represent either z or w, depending on which variable we are referring to in the subsequent discussion. Focusing on the later case, it holds that

$$\begin{aligned}&sgn(z(t_j,x)-z(t,x))(\tfrac{\partial}{\partial t}(z(t_j,x)-z(t,x)))\\&\quad\leq sgn(z(t_j,x)-z(t,x))\Big(\lambda_1 z_x(t,x)+\kappa a w(t,x)+b_1 d^*(t,x)\Big)\end{aligned} \tag{3.46}$$

and

$$sgn(w(t_j,x)-w(t,x))\left(\frac{\partial}{\partial t}(w(t_j,x)-w(t,x))\right) \leq sgn(w(t_j,x)-w(t,x))\Big(-\lambda_2 w_x(t,x)+\kappa w(t,x)+b_2 d^*(t,x)\Big). \tag{3.47}$$

If $x \in I(t)\cap(0,1)$ and satisfies $(z(t_j,x)-z(t,x)) = \|z(t_j,\cdot)-z(t,\cdot)\|_\infty$, $(w(t_j,x)-w(t,x)) = \|w(t_j,\cdot)-w(t,\cdot)\|_\infty$ then $(z(t_j,x)-z(t,x))$ and $(w(t_j,x)-w(t,x))$ have a maximum at x, hence $z_x(t_j,x) = z_x(t,x)$, $w_x(t_j,x) = w_x(t,x)$ and $z(t,x) = z(t_j,x)-\|z(t_j,\cdot)-z(t,\cdot)\|_\infty$, and $w(t,x) = w(t_j,x)-\|w(t_j,\cdot)-w(t,\cdot)\|_\infty$. Hence,

$$sgn(z(t_j,x)-z(t,x))\frac{\partial}{\partial t}(z(t_j,x)-z(t,x)) \leq \lambda_1 z_x(t_j,x)+\kappa a w(t_j,x)-\kappa a\|w(t_j,\cdot)-w(t,\cdot)\|_\infty+b_1 d^*(t,x) \tag{3.48}$$

and

$$sgn(w(t_j,x)-w(t,x))\frac{\partial}{\partial t}(w(t_j,x)-w(t,x)) \leq \lambda_2 w_x(t_j,x)-\kappa w(t_j,x)-\kappa\|w(t_j,\cdot)-w(t,\cdot)\|_\infty+b_2 d^*(t,x). \tag{3.49}$$

If $x \in I(t)\cap(0,1)$ and satisfies $(z(t_j,x)-z(t,x)) = -\|z(t_j,\cdot)-z(t,\cdot)\|_\infty$, $(w(t_j,x)-w(t,x)) = -\|w(t_j,\cdot)-w(t,\cdot)\|_\infty$ then $(z(t_j,x)-z(t,x))$ and $(w(t_j,x)-w(t,x))$ have a minimum at x, hence $z_x(t_j,x) = z_x(t,x)$, $w_x(t_j,x) = w_x(t,x)$ and $z(t,x) = z(t_j,x)+\|z(t_j,\cdot)-z(t,\cdot)\|_\infty$, and $w(t,x) = w(t_j,x)+\|w(t_j,\cdot)-w(t,\cdot)\|_\infty$. Thus,

$$sgn(z(t_j,x)-z(t,x))\frac{\partial}{\partial t}(z(t_j,x)-z(t,x)) \leq \lambda_1 z_x(t_j,x)+\kappa a w(t_j,x)+\kappa a\|w(t_j,\cdot)-w(t,\cdot)\|_\infty+b_1 d^*(t,x) \tag{3.50}$$

and

$$sgn(w(t_j,x)-w(t,x))\frac{\partial}{\partial t}(w(t_j,x)-w(t,x)) \leq \lambda_2 w_x(t_j,x)-\kappa w(t_j,x)+\kappa\|w(t_j,\cdot)-w(t,\cdot)\|_\infty+b_2 d^*(t,x). \tag{3.51}$$

Combining both cases, and using (3.37) we obtain

$$\begin{aligned}\frac{d\|z(t_j,\cdot)-z(t,\cdot)\|_\infty}{dt} &\leq |\lambda_1|\|z_x(t_j,\cdot)\|_\infty+|\kappa a|\|w(t_j,\cdot)\|_\infty+|\kappa a|\|w(t_j,\cdot)-w(t,\cdot)\|_\infty+|b_1|\|d^*(t,\cdot)\|_\infty\\ &\leq |\lambda_1|\|z_x(t_j,\cdot)\|_\infty+|\kappa a|\|w(t_j,\cdot)\|_\infty+|\kappa a|\|w(t_j,\cdot)-w(t,\cdot)\|_\infty\\ &\quad+|\kappa|\|z(t_j,\cdot)\|_\infty+|\kappa|\|z(t_j,\cdot)-z(t,\cdot)\|_\infty\\ &\quad+|b_1|R\Big(\|z(t_j,\cdot)-z(t,\cdot)\|_\infty+\|w(t_j,\cdot)-w(t,\cdot)\|_\infty\Big),\end{aligned} \tag{3.52}$$

and

$$\begin{aligned}\frac{d\|w(t_j,\cdot)-w(t,\cdot)\|_\infty}{dt} &\le |\lambda_2|\|w_x(t_j,\cdot)\|_\infty + |\kappa|\|w(t_j,\cdot)\|_\infty + |\kappa|\|w(t_j,\cdot)-w(t,\cdot)\|_\infty + |b_2|\|d^*(t,\cdot)\|_\infty \\ &\le |\lambda_2|\|w_x(t_j,\cdot)\|_\infty + |\kappa|\|w(t_j,\cdot)\|_\infty + |\kappa|\|w(t_j,\cdot)-w(t,\cdot)\|_\infty \\ &\quad + |b_2|R\Big(\|z(t_j,\cdot)-z(t,\cdot)\|_\infty + \|w(t_j,\cdot)-w(t,\cdot)\|_\infty\Big). \end{aligned} \tag{3.53}$$

Therefore, using (3.37),(3.40) and (3.41) we have from (3.52) and (3.53) that

$$\dot{\psi}(t) \le \big(\bar{K} + R(|b_1| + |b_2|)\big)\,\psi(t) + \chi(t_j), \tag{3.54}$$

for $t \in (t_j, t_{j+1})$, where $\chi(\cdot)$ (depending on the current state at sampled time $t = t_j$) is a constant quantity defined as follows:

$$\chi(t_j) := \frac{1}{\min\left(\frac{\beta_1}{R+\beta_1}\cdot\frac{\beta_2}{R+\beta_2}\right)}\left(\bar{K} + \bar{\lambda}\left(\frac{\|z_x(t_j,\cdot)\|_\infty + \|w_x(t_j,\cdot)\|_\infty}{\|z(t_j,\cdot)\|_\infty + \|w(t_j,\cdot)\|_\infty}\right)\right) > 0, \tag{3.55}$$

with $\bar{\lambda} = \max(\lambda_1, \lambda_2)$ and $\bar{K} = \kappa \max(|a+1|, 1)$.

Then, by the comparison principle, it follows that the time needed by ψ to go from $\psi(t_j) = 0$ to $\psi(t_{j+1}^-) = 1$ is at least

$$\begin{aligned} T_j &= \frac{1}{\bar{K} + R(|b_1| + |b_2|)} \ln\left(1 + \frac{\bar{K} + R(|b_1| + |b_2|)}{\chi(t_j)}\right) \\ &\ge \frac{1}{\chi(t_j) + \bar{K} + R(|b_1| + |b_2|)} > 0, \quad \forall j \ge 0, \end{aligned} \tag{3.56}$$

where we have used the property $\ln(s) \ge \frac{s-1}{s}$.

In particular, notice that the first inter-sampling interval is lower bounded by $T_0 \ge \frac{1}{\chi(0)+\bar{K}+R(|b_1|+|b_2|)} > 0$. This concludes the proof. □

Theorem 2 allows to conclude that $\lim_{j\to\infty}(t_j) = \infty$. Consequently, we derive the following corollary, which states the exponential stability result.

COROLLARY 1. Let $\beta_1, \beta_2 > 0$ (design parameters involved in the triggering condition (3.1)) that are selected such that (3.10) holds. Let ς be such that (3.11) holds. Then, for any initial conditions $(z_0, w_0) \in (L^\infty(0,1))^2$, $\eta(0) \in \mathbb{R}$, the closed-loop system (2.26)–(2.30) with ETC (2.25), (3.1) is exponentially stable, that is, there exists a constant $\Theta > 0$ such that the following estimate holds:

$$\|z(t,\cdot)\|_\infty + \|w(t,\cdot)\|_\infty + |\eta(t)| \le \Theta \exp(-\varsigma t)\Big(\|z_0\|_\infty + \|w_0\|_\infty + |\eta(0)|\Big) \tag{3.57}$$

for all $t \ge 0$.

Proof. It is a consequence of Theorem 2 in conjunction with Theorem 1. □

Corollary 1 holds, in particular, if we set the initial conditions as in (2.23) and $\eta(0) = w(0,1)$.

REMARK 2. The bound (3.56) obtained in the proof of Theorem 2 shows that any inter-sampling interval is lower bounded by a positive constant. However, there is a dependence on j, and therefore we lack uniformity. From (3.56), it may not be straightforward to obtain a minimal dwell-time, uniform, independent of j and the system's initial conditions.

REMARK 3. By examining the bound (3.56), we observe that the proof of Theorem 2 naturally suggests an *STC strategy*. In STC strategies, the next triggering time is computed based on the state information at the current sampling time t_j, eliminating the need for continuous monitoring of the triggering condition. This approach has been extensively studied for finite-dimensional systems (Heemels *et al.*, 2012; Liu *et al.*, 2020) (see also the survey Zhang *et al.* (2023)), but remains relatively unexplored for PDEs. Notable exceptions include some recent developments in STC for PDEs, such as the strategies proposed for a class of reaction-diffusion PDEs (Rathnayake & Diagne, 2024) and subsequently for 2×2 boundary-controlled hyperbolic PDEs (Somathilake *et al.*, 2024).

In our case, we could also propose an STC strategy based on the sup-norm of the state and its spatial variation, both at the current sampling time t_j, which would be given by

$$t_{j+1} = t_j + \frac{1}{\chi(t_j) + \bar{K} + R(|b_1| + |b_2|)}, \tag{3.58}$$

where $\chi(t_j)$ is defined by (3.55). However, studying STC strategies for our problem requires a thorough analysis, particularly to assess the conservatism of the approach (as our current bounds are quite conservative) and to avoid $\chi(t_j)$ being dependent on the spatial variation of the solution. Instead, we aim to rely solely on the norm of the state at the previous sampling time to make the self-triggered strategy more feasible for implementation. These considerations warrant deeper investigation but are beyond the scope of this paper.

4. Numerical simulations

In this section, we present a numerical example to demonstrate the validity of our results. We perform simulations on system (2.26)–(2.30) with control (2.25), (3.1) by employing a two-step LxF method (Shampine, 2005b) that can be set in Shampine's solver for Matlab detailed in Shampine (2005a). The spatial and temporal discretization were done with steps $\Delta x = 1.4 \times 10^{-3}$ and $\Delta t = 0.2$. It can be verified that the Courant–Friedrich–Levy condition for the numerical stability holds. Then, we obtain the numerical solutions of (2.1)–(2.4) via the change of variables (2.17)–(2.18) along with (2.12). We run simulations on a time horizon $T = 400$ s. The initial conditions are chosen as $\rho(0,\bar{x}) = \bar{\rho} + 10\cos\left(\frac{8\pi\bar{x}}{L}\right)$, and $v(0,\bar{x}) = \frac{q_{\text{in}}}{\rho(0,\bar{x})}$ (thus $z(0,x) = \frac{\bar{v}}{\bar{\rho}}\left(10\cos(8\pi x) + \frac{\bar{h}_{\text{mix}}\,\bar{\rho}}{(l+\bar{h}_{\text{mix}}\bar{v})}\left(\frac{q_{\text{in}}}{\bar{\rho}+10\cos(8\pi x)} - \bar{v}\right)\right)$, $w(0,x) = \frac{q_{\text{in}}}{\bar{\rho}+10\cos(8\pi x)} - \bar{v}$ and $\eta(0) = w(0,1)$ for system (2.26)–(2.30), according to (2.17)–(2.18) along with (2.12)).

The traffic parameters of the system (2.1)–(2.4) are given in Table 2 and are borrowed from (Bekiaris-Liberis & Delis, 2021, section V).

TABLE 2 *Parameters of the system (2.1)–(2.4) chosen as in Bekiaris-Liberis & Delis (2021)*

$\bar{\rho} = 105.8[\frac{\text{veh}}{\text{km}}]$	$\bar{v} = 11.35[\frac{\text{km}}{\text{h}}]$	$\tau_{acc} = 2[\text{s}]$	$\bar{h}_{mix} = 1.39[\text{s}]$
$q_{\text{in}} = 1200[\frac{\text{veh}}{\text{h}}]$	$L = 1000[\text{m}]$	$\tau_m = 60[\text{s}]$	$h_m = 1[s]$
$\rho_{min} = 37[\frac{\text{veh}}{\text{km}}]$	$l = 5[\text{m}]$	$\alpha = 0.15$	$\bar{h}_{acc} = 1.5[\text{s}]$

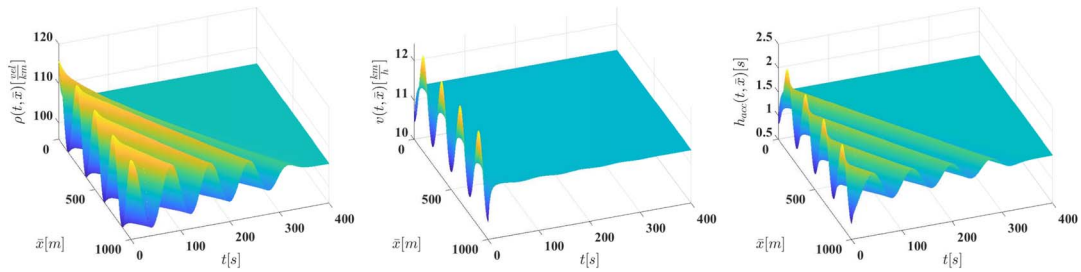

FIG. 2. Numerical solution of ρ and v in system (2.1)–(2.4), and profile of the nominal controller (2.24) (under the original variables via (2.17)–(2.18)).

The control gain κ (see (2.25)) is set as $\kappa = 0.25[\frac{1}{s}]$, as in Bekiaris-Liberis & Delis (2021). The parameters of the triggering condition (3.1) are tuned to $\beta_1 = 9 \times 10^{-4}$ and $\beta_2 = 0.118$, verifying (3.10). The tuning of those parameters can be done using e.g. a 'line search' (by increasing progressively β_1 and β_2) until condition (3.10) is no longer verified.

However, it is important to emphasize that due to the conservatism of our proposed approach (small-gain based ETC design), the parameters β_1 and β_2 turn out to be very small. This implies that when implementing the ETC strategy, the resulting numerical solution of the closed-loop system would behave similar as in the continuous case (i.e. under a nominal control—see Fig. 2), since the updating of the event-triggered controller occurs very often. See also Remark 1. The theoretical results, although conservative, allow to study qualitatively the behaviour of the system under an event-triggered strategy and the robustness to sampling. Now, in practice we can select larger values of β_1 and β_2 that violate the small-gain condition (3.10), and still observe, numerically, convergence of the solution of system to the desired profiles. For instance, we can set $\beta_1 = 0.19$ and $\beta_2 = 0.82$, which imply less updating of the controller, and yet observe the convergence of the closed-loop solutions. Indeed, Fig. 3 shows the numerical solution of system (2.1)–(2.4) in closed loop under the ETC (2.25), (3.1). Figure 4 shows the profile at the boundary $\bar{x} = L$, of the ETC (2.25) and the nominal control (2.24) (under the original variables via (2.17)–(2.18)).

Figure 5 shows the time evolution of the sup-norms of the the linear hyperbolic system (2.26)–(2.30) using small-gain event-triggered controller (2.25) (red line), and the nominal continuous controller (2.24) (blue line). In both cases, we can observe exponential convergence to zero, and it can be highlighted a better performance (in terms of convergence rate) under a nominal controller, as expected.

Finally, we investigate traffic system performance, by computing the following metrics, introduced in Treiber & Kesting (2013); these are, respectively, the fuel consumption J_{fuel}, travel comfort J_{comfort}

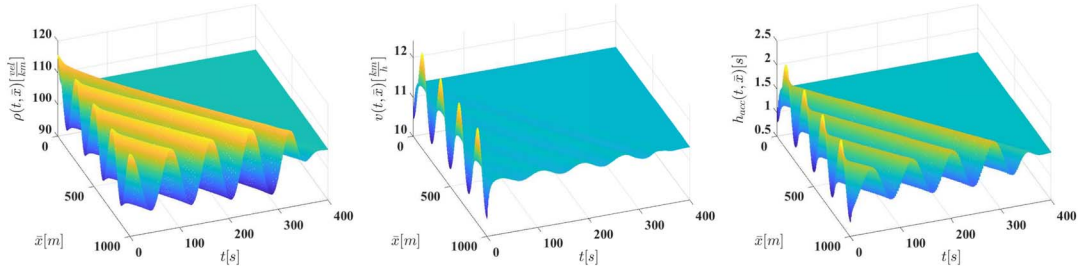

FIG. 3. Numerical solution of ρ and v in system (2.1)–(2.4), and profile of the small-gain event-triggered controller (2.25), (3.1) with $\beta_1 = 0.19$ and $\beta_2 = 0.82$.

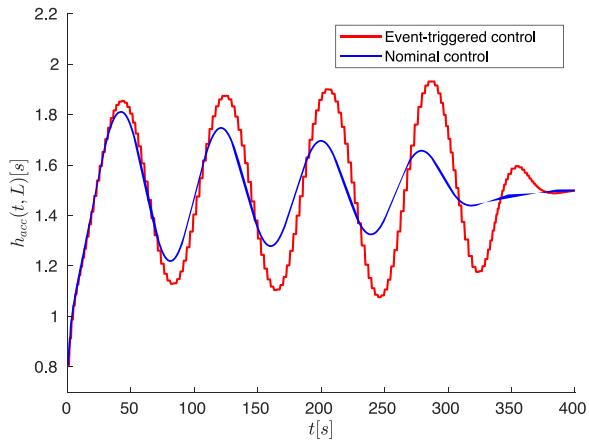

FIG. 4. Profile at the boundary $\bar{x} = L$ of the ETC (2.25) (red line) and the nominal control (2.24) (blue line)—both under the original variables via (2.17)–(2.18).

and total travel time J_{TTT}:

$$J_{\text{fuel}} = \int_0^T \int_0^L \max\{0, \delta_0 + \delta_1 v(t,\bar{x}) + \delta_3 v(t,\bar{x})^3 + \delta_4 v(t,\bar{x})\bar{a}(t,\bar{x})\}\rho(t,\bar{x})d\bar{x}dt, \tag{4.1}$$

$$J_{\text{comfort}} = \int_0^T \int_0^L \left(\bar{a}(t,\bar{x})^2 + \bar{a}_t(t,\bar{x})^2\right)\rho(t,\bar{x})d\bar{x}dt, \tag{4.2}$$

$$J_{\text{TTT}} = \int_0^T \int_0^L \rho(t,\bar{x})d\bar{x}dt, \tag{4.3}$$

where $\bar{a}(t,\bar{x}) = v_t(t,\bar{x}) + v(t,\bar{x})v_{\bar{x}}(t,\bar{x})$ is the local acceleration, and the following parameters: $\delta_0 = 25 \times 10^{-3}$[1/s], $\delta_1 = 24.5 \times 10^{-6}$[1/m], $\delta_3 = 32.5 \times 10^{-9}$[1s^3/m^2] and $\delta_4 = 125.6 \times 10^{-6}$[1s^2/m^2]. For more details, we refer to (Treiber & Kesting, 2013, page 485).

We compare the traffic performance metrics in open loop with the performance metrics obtained in closed loop under both the nominal continuous-time control (given in (2.24)) and the ETC (given in (2.25),(3.1)) strategies. Table 3 reports the percentage of improvement with respect to the

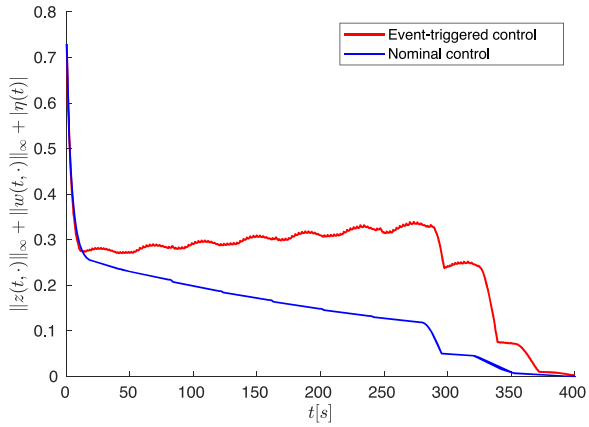

FIG. 5. Time-evolution of the sup-norms of the linear hyperbolic system (2.26)–(2.30) under small-gain event-triggered controller (2.25) (red line), and the nominal continuous controller (2.24) (blue line).

TABLE 3 *Performance indices (4.1)–(4.3)*

Performance index	**Improvement (%) with nominal control (2.24)**	**Improvement (%) with ETC (2.25)**
J_{fuel}	5.928	5.928
J_{comfort}	96.48	76.53
J_{TTT}	5.962	5.967

open-loop driving behaviour. Closing the loop with a feedback controller considerably improves all fuel consumption, total travel time and drivers' comfort compared with the open-loop scenario. It is worth noticing, however, that the ETC strategy leads the drivers to experience more discomfort, yet much lower than if no control is applied at all. Overall, application of ETC results in better performance in all of the metrics, compared with the open-loop baseline.

5. Conclusion

This paper proposed an ETC scheme to regulate mixed traffic flow, incorporating ACC-equipped vehicles, under the ARZ-type modelling framework. The event-triggered scheme makes use of a small-gain based triggering condition. We performed the stability analysis through ISS estimates and small-gain arguments. The ETC design ensures exponential stability in the supr-norm, and we prove the avoidance of the Zeno phenomenon (though lacking uniformity as there is dependence on the information of the current inter-sampling interval). Future work will focus on reducing the frequency of updating by addressing the conservativeness of the event-triggering conditions, thereby improving system efficiency and further optimizing the control strategy. To this end, we will rely on recent strategies such as performance-barrier-based ETC (Zhang *et al.*, 2025). In addition, spatial discretization can also be studied based on recent advancements in sampled-data control of mixed traffic flow by Zhao *et al.* (2024).

Acknowledgements

The work of the first author was partially supported by the Hauts-de-France region under the project RITMEA. The work of the second and third authors was partially supported by the Agence Nationale dela Recherche (ANR) via grant PH-DIPSY ANR-24-CE48-1712. The work of the last author was fundedby the European Union (ERC, C-NORA, 101088147). Views and opinions expressed are, however,those of the authors only and do not necessarily reflect those of the European Union or the European Research Council. Neither the European Union nor the granting authority can be held responsible for them.

References

Alan, A., He, C. R., Molnar, T. G., Mathew, J. C., Bell, A. H. & Orosz, G. (2023) Integrating safety with performance in connected automated truck control: experimental validation. *IEEE Tran. Intell. Veh.*, **9**, 3075–3088.

Aw, A. & Rascle, M. (2000) Resurrection of 'second order' models of traffic flow. *SIAM J. Appl. Math.*, **60**, 916–938.

Bayen, A., Coron, J. M., De Nitti, N., Keimer, A. & Pflug, L. (2021) Boundary controllability and asymptotic stabilization of a nonlocal traffic flow model. *Vietnam J. Math.*, **49**, 957–985.

Bayen, A., Delle Monache, M. L., Garavello, M., Goatin, P. & Piccoli, B. (2022) *Control Problems for Conservation Laws with Traffic Applications: Modeling, Analysis, and Numerical Methods*. Cham: Springer International Publishing.

Bekiaris-Liberis, N. & Delis, A. I. (2021) PDE-based feedback control of freeway traffic flow via time-gap manipulation of ACC-equipped vehicles. *IEEE Trans. Control Syst. Technol.*, **29**, 461–469.

Bose, A. & Ioannou, P. (2003) Mixed manual/semi-automated traffic: a macroscopic analysis. *Transp. Res. Part C Emerging Technol.*, **11**, 439–462.

Chen, Y., Orosz, G. & Molnar, T. G. (2024) Safe and stable connected cruise control for connected automated vehicles with response lag. arXiv:2409.06884.

Darbha, S. & Rajagopal, K. (1999) Intelligent cruise control systems and traffic flow stability. *Transp. Res. Part C Emerging Technol.*, **7**, 329–352.

Diagne, M. & Karafyllis, I. (2021) Event-triggered boundary control of a continuum model of highly re-entrant manufacturing systems. *Automatica*, **134**, 109902.

Espitia, N. (2020) Observer-based event-triggered boundary control of a linear 2×2 hyperbolic systems. *Syst. Control Lett.*, **138**, 104668.

Espitia, N., Girard, A., Marchand, N. & Prieur, C. (2018) Event-based boundary control of a linear 2x2 hyperbolic system via backstepping approach. *IEEE Trans. Autom. Control*, **63**, 2686–2693.

Espitia, N., Yu, H. & Krstic, M. (2020) Event-triggered varying speed limit control for stop-and-go traffic. *Proc of the IFAC World Congress*, **53**, 7509–7514.

Espitia, N., Karafyllis, I. & Krstic, M. (2021) Event-triggered boundary control of constant-parameter reaction-diffusion PDEs: a small gain approach. *Automatica*, **128**, 109562.

Espitia, N., Auriol, J., Yu, H. & Krstic, M. (2022) Traffic flow control on cascaded roads by event-triggered output feedback. *Int. J. Robust Nonlinear Control*, **32**, 5919–5949.

Goatin, P., Göttlich, S. & Kolb, O. (2016) Speed limit and ramp meter control for traffic flow networks. *Eng. Optim.*, **48**, 1121–1144.

Heemels, W.P.M.H., Johansson, K.H. & Tabuada, P. (2012) *IEEE Conference on Decision and Control (CDC)*, An introduction to event-triggered and self-triggered control. Hawaii, USA, p. 3270–3285.

Karafyllis, I. & Krstic, M. (2018) *Input-to-State Stability for PDEs*. Cham, Switzerland: Springer.

Karafyllis, I. & Krstic, M. (2021) ISS estimates in the spatial sup-norm for nonlinear 1-D parabolic PDEs. *ESAIM: COCV*, **27**, 1–23.

Karafyllis, I., Bekiaris-Liberis, N. & Papageorgiou, M. (2018) Feedback control of nonlinear hyperbolic PDE systems inspired by traffic flow models. *IEEE Trans. Autom. Control*, **64**, 3647–3662.

Katz, R., Fridman, E. & Selivanov, A. (2021) Boundary delayed observer-controller design for reaction–diffusion systems. *IEEE Trans. Autom. Control*, **66**, 275–282.

Koudohode, F., Espitia, N. & Krstic, M. (2024) Event-triggered boundary control of an unstable reaction diffusion PDE with input delay. *Syst. Control Lett.*, **186**, 105775.

Li, J., Yu, C., Shen, Z., Su, Z. & Ma, W. (2023) A survey on urban traffic control under mixed traffic environment with connected automated vehicles. *Transp. Res. Part C Emerging Technol.*, **154**, 104258.

Liu, T., Zhang, P. & Jiang, Z.-P. (2020) *Robust Event-Triggered Control of Nonlinear Systems*. Springer Singapore: Springer.

Manolis, D., Spiliopoulou, A., Vandorou, F. & Papageorgiou, M. (2020) Real time adaptive cruise control strategy for motorways. *Transp. Res. Part C Emerging Technol.*, **115**, 102617.

Molnar, T. G. & Orosz, G. (2024) Destroying phantom jams with connectivity and automation: nonlinear dynamics and control of mixed traffic. *Transp. Sci.*, **58**, 1319–1334.

Papageorgiou, M. (1980) A new approach to time-of-day control based on a dynamic freeway traffic model. *Transp. Res. Part B: Methodol.*, **14**, 349–360.

Papageorgiou, M. (1995) An integrated control approach for traffic corridors. *Transp. Res. Part C Emerging Technol.*, **3**, 19–30.

Payne, H. J. (1971) Model of freeway traffic and control. Bekey G.A. (ed.), *Mathematical Models of Public System*, La Jolla, California, USA: Simulation Councils, Inc. 51–61.

Prieur, C., Girard, A. & Witrant, E. (2014) Stability of switched linear hyperbolic systems by Lyapunov techniques. *IEEE Trans. Autom. Control*, **59**, 2196–2202.

Qi, J., Mo, S. & Krstic, M. (2023) Delay-compensated distributed PDE control of traffic with connected/automated vehicles. *IEEE Trans. Autom. Control*, **68**, 2229–2244.

Rathnayake, B. & Diagne, M. (2024) Observer-based periodic event-triggered and self-triggered boundary control of a class of parabolic PDEs. *IEEE Trans. Autom. Control*, **69**, 8836–8843.

Rathnayake, B., Diagne, M., Espitia, N. & Karafyllis, I. (2021) Observer-based event-triggered boundary control of a class of reaction–diffusion PDEs. *IEEE Trans. Autom. Control*, **67**, 2905–2917.

Rathnayake, B., Diagne, M., Cortes, J. & Krstic, M. (2024) Performance-barrier-based event-triggered boundary control of a class of reaction-diffusion PDEs. *Proceedings of the 2024 American Control Conference (ACC)*. Toronto, Ontario, Canada: IEEE, pp. 5313–5319.

Selivanov, A. & Fridman, E. (2016) Distributed event-triggered control of transport-reaction systems. *Automatica*, **68**, 344–351.

Shampine, L. F. (2005a) Solving hyperbolic PDEs in MATLAB. *Appl. Numer. Anal. Comput. Math.*, **2**, 346–358.

Shampine, L. F. (2005b) Two-step Lax–Friedrichs method. *Appl. Math. Lett.*, **18**, 1134–1136.

Somathilake, E., Rathnayake, M. & Diagne, B. (2024) Output feedback periodic-event and self-triggered control of coupled 2×2 linear hyperbolic PDEs. Automatica, **179**, 2025.

Strecker, T., Cantoni, M. & Aamo, O. M. (2024) Event-triggered boundary control of 2×2 semilinear hyperbolic systems. *IEEE Trans. Autom. Control*, **68**, 418–425.

Tabuada, P. (2007) Event-triggered real-time scheduling of stabilizing control tasks. *IEEE Trans. Autom. Control*, **52**, 1680–1685.

Treiber, M. & Kesting, A. (2013) *Traffic Flow Dynamics–Data, Models and Simulation*. Berlin, Heidelberg: Springer Berlin Heidelberg.

Wang, J. & Krstic, M. (2021) Adaptive event-triggered PDE control for load-moving cable systems. *Automatica*, **129**, 109637.

Wang, X., Tang, Y., Espitia, N. & Bekiaris-Liberis, N. (2025) Event-triggered control of freeway traffic flow with connected and automated vehicles. *5th IFAC Workshop on Control of Systems Governed by Partial Differential Equations (CPDE 2025)*, Beijing, China.

Whitham, G. B. (1974) *Linear and Nonlinear Waves*. New York, NY: John Wiley & Sons.

Yi, J. & Horowitz, R. (2006) Macroscopic traffic flow propagation stability for adaptive cruise controlled vehicles. *Transp. Res. Part C Emerging Technol.*, **14**, 81–95.

Yu, H. & Krstic, M. (2019) Traffic congestion control for Aw-Rascle-Zhang model. *Automatica*, **100**, 38–51.

Yu, L. & Wang, R. (2022) Researches on adaptive cruise control system: a state of the art review. *Proc. Inst. Mech. Eng. Part D: J. Automob. Eng.*, **236**, 211–240.
Zhang, H. M. (2002) A non-equilibrium traffic model devoid of gas-like behavior. *Transp. Res. Part B Methodol.*, **36**, 275–290.
Zhang, Y. & Yu, H. (2024) Event-triggered boundary control of mixed-autonomy traffic. arXiv preprint-arXiv:2403.14194.
Zhang, P., Liu, T., Chen, J. & Jiang, Z.-P. (2023) Recent developments in event-triggered control of nonlinear systems: an overview. *Unmanned Syst.*, **11**, 27–56.
Zhang, Y., Yu, H., Auriol, J. & Pereira, M. (2024) Mean-square exponential stabilization of mixed-autonomy traffic PDE system. *Automatica*, **170**, 111859.
Zhang, P., Rathnayake, B., Diagne, M. & Krstic, M. (2025) Performance-barrier event-triggered PDE control of traffic flow. *IEEE Tran. Autom. Control*, **70**, 5720–5735.
Zhao, H., Zhan, J. & Zhang, L. (2024) Sampled-data distributed control of mixed traffic flow with ACC-equipped vehicles (I). *2024 IEEE 63th Conference on Decision and Control (CDC)*, Milan, Italy.

A. Appendix

A.1. *Proof of Lemma 1*

By the method of characteristics, the explicit solution of (2.33) with boundary condition (2.35) and initial data $z(0,x)$, $x \in [0,1]$, is given as follows, for all $t \in [0, \lim_{j\to\infty}(t_j))$:

$$z(t,x) = z\left(0, x-\lambda_1 t\right) + \int_0^t (-\kappa a) w(\tau, x-\lambda_1 t+\lambda_1\tau)d\tau + \int_0^t (-b_1) d^*(\tau, x-\lambda_1 t+\lambda_1\tau)d\tau, \quad \text{(A.1)}$$

for $0 \le t \le \frac{x}{\lambda_1}$, and

$$z(t,x) = -rw\left(t-\tfrac{1}{\lambda_1}x, 0\right) + \int_{t-\frac{x}{\lambda_1}}^t (-\kappa a) w(\tau, x-\lambda_1 t+\lambda_1\tau)d\tau + \int_{t-\frac{x}{\lambda_1}}^t (-b_1) d^*(\tau, x-\lambda_1 t+\lambda_1\tau)d\tau, \quad \text{(A.2)}$$

for $\frac{x}{\lambda_1} \le t$. From (A1) and (A2), the solution can be seen as the sum of the following terms for all $t \in [0, \lim_{j\to\infty}(t_j))$:

$$z(t,x) = \bar{z}_1(t,x) + \bar{z}_2(t,x) + \bar{z}_3(t,x) + \bar{z}_4(t,x), \quad \text{(A.3)}$$

where

$$\bar{z}_1(t,x) := z\left(0, x-\lambda_1 t\right), \quad \text{(A4)}$$

$$\bar{z}_2(t,x) := 0, \quad \text{(A5)}$$

$$\bar{z}_3(t,x) := \int_0^t (-b_1) d^*(\tau, x-\lambda_1 t+\lambda_1\tau)d\tau, \quad \text{(A6)}$$

$$\bar{z}_4(t,x) := \int_0^t (-\kappa a) w(\tau, x-\lambda_1 t+\lambda_1\tau)d\tau, \quad \text{(A7)}$$

for $t \in [0, \lim_{j\to\infty}(t_j)), x \in [0,1]$ with $0 \le t \le \frac{x}{\lambda_1}$, and

$$\bar{z}_1(t,x) := 0, \tag{A8}$$

$$\bar{z}_2(t,x) := -rw\left(t - \tfrac{1}{\lambda_1}x, 0\right), \tag{A9}$$

$$\bar{z}_3(t,x) := \int_{t-\frac{x}{\lambda_1}}^{t} (-b_1) d^*(\tau, x - \lambda_1 t + \lambda_1 \tau) d\tau, \tag{A10}$$

$$\bar{z}_4(t,x) := \int_{t-\frac{x}{\lambda_1}}^{t} (-\kappa a) w(\tau, x - \lambda_1 t + \lambda_1 \tau) d\tau, \tag{A11}$$

for $t \in [0, \lim_{j\to\infty}(t_j)), x \in [0,1]$ with $\frac{x}{\lambda_1} \le t$. We estimate the $L^p(0,1)$ norm of $\bar{z}_1$, with $p \in [1,\infty)$. From (A4), the following estimate holds for every $\varsigma > 0$:

$$\begin{aligned}
\left|\bar{z}_1(t,x)\right|^p &= \left|z\left(0, x - \lambda_1 t\right)\right|^p \\
&\le e^{-p\varsigma t} e^{p\varsigma \frac{x}{\lambda_1}} \left|z\left(0, x - \lambda_1 t\right)\right|^p \\
&\le e^{-p\varsigma t} e^{p\varsigma \frac{1}{\lambda_1}} \left|z\left(0, x - \lambda_1 t\right)\right|^p.
\end{aligned}$$

Therefore, we get

$$\left\|\bar{z}_1(t,\cdot)\right\|_{L^p} \le e^{-\varsigma t} e^{\frac{\varsigma}{\lambda_1}} \left\|z(0,\cdot)\right\|_{L^p}. \tag{A.12}$$

We estimate the $L^p(0,1)$ norm of $\bar{z}_2$, with $p \in [1,\infty)$. From (A9), the following estimate holds for every $\varsigma > 0$:

$$\begin{aligned}
\left|\bar{z}_2(t,x)\right|^p &= |r|^p \left|w\left(t - \tfrac{1}{\lambda_1}x, 0\right)\right|^p \\
&= e^{p\varsigma \frac{x}{\lambda_1}} e^{-p\varsigma\left(t-\left(t-\frac{x}{\lambda_1}\right)\right)} |r|^p \left|w\left(t - \tfrac{1}{\lambda_1}x, 0\right)\right|^p \\
&\le e^{p\varsigma \frac{x}{\lambda_1}} |r|^p \max_{t-\frac{1}{\lambda_1} \le s \le t} \left(|w(s,0)|^p e^{-p\varsigma(t-s)}\right) \\
&\le e^{p\varsigma \frac{1}{\lambda_1}} |r|^p \max_{\max\left\{0, t-\frac{1}{\lambda_1}\right\} \le s \le t} \left(|w(s,0)|^p e^{-p\varsigma(t-s)}\right),
\end{aligned} \tag{A.13}$$

for all $t \in [0, \lim_{j\to\infty}(t_j))$, $x \in [0,1]$ with $\frac{x}{\lambda_1} \le t$. Hence, we obtain for every $\varsigma > 0$, $p \in [1,\infty)$ and $t \in [0, \lim_{j\to\infty}(t_j))$

$$\left\|\bar{z}_2(t,\cdot)\right\|_{L^p} \le e^{\varsigma \frac{1}{\lambda_1}} |r| \max_{\max\left\{0, t-\frac{1}{\lambda_1}\right\} \le s \le t} \left(|w(s,0)|\, e^{-\varsigma(t-s)}\right). \tag{A.14}$$

Using Lyapunov analysis, we estimate the $L^p(0,1)$ norm of $\bar{z}_3$, which verifies $\bar{z}_{3t}(t,x) = -\lambda_1 \bar{z}_{3x}(t,x) - \kappa a w(t,x) - b_1 d^*(t,x)$ based on (2.33) with $\bar{z}_3(t,0) = 0$ for $t \in [0, \lim_{j\to\infty}(t_j))$, and the initial data

$\bar{z}_3(0,x) = 0$ for all $x \in [0,1]$. Let us define

$$V_1(\bar{z}_3) = \int_0^1 e^{-\mu x} |\bar{z}_3(t,x)|^p dx, \tag{A.15}$$

with $\mu > 0$ to be selected in the sequel. Computing the time derivative, we have

$$\begin{aligned}\dot{V}_1(\bar{z}_3) &= p \int_0^1 e^{-\mu x} sign(\bar{z}_3(t,x)) \bar{z}_{3t}(t,x) |\bar{z}_3(t,x)|^{p-1} dx \\ &= p \int_0^1 e^{-\mu x} sign(\bar{z}_3(t,x)) \left[-\lambda_1 \bar{z}_{3x}(t,x) - \kappa a w(t,x) - b_1 d^*(t,x) \right] |\bar{z}_3(t,x)|^{p-1} dx. \end{aligned} \tag{A.16}$$

Since the following holds:

$$\begin{aligned} & p \int_0^1 e^{-\mu x} sign(\bar{z}_3(t,x)) \left(-\lambda_1 \bar{z}_{3x}(t,x) \right) |\bar{z}_3(t,x)|^{p-1} dx \\ &= -\lambda_1 \left[e^{-\mu x} |\bar{z}_3(t,x)|^p \right]_0^1 - \int_0^1 e^{-\mu x} \mu \lambda_1 |\bar{z}_3(t,x)|^p dx \\ &= -\lambda_1 e^{-\mu} |\bar{z}_3(t,1)|^p + \lambda_1 |\bar{z}_3(t,0)|^p - \mu \lambda_1 V_1(\bar{z}_3), \end{aligned} \tag{A.17}$$

and using the Young's inequality,

$$|\bar{z}_3(t,x)|^{p-1} w(t,x) \le \frac{p-1}{p} \epsilon_0^{\frac{p}{p-1}} |\bar{z}_3(t,x)|^p + \frac{1}{p} \epsilon_0^{-p} |w(t,x)|^p, \tag{A18}$$

$$|\bar{z}_3(t,x)|^{p-1} d^*(t,x) \le \frac{p-1}{p} \epsilon_1^{\frac{p}{p-1}} |\bar{z}_3(t,x)|^p + \frac{1}{p} \epsilon_1^{-p} |d^*(t,x)|^p, \tag{A19}$$

we obtain, from (A16)–(A19),

$$\begin{aligned} \dot{V}_1(\bar{z}_3) \le & - \mu \lambda_1 V_1(\bar{z}_3) + |\kappa a| (p-1) \epsilon_0^{\frac{p}{p-1}} \int_0^1 e^{-\mu x} |\bar{z}_3(t,x)|^p dx + |\kappa a| \epsilon_0^{-p} \int_0^1 e^{-\mu x} |w(t,x)|^p dx \\ & + |b_1| (p-1) \epsilon_1^{\frac{p}{p-1}} \int_0^1 e^{-\mu x} |\bar{z}_3(t,x)|^p dx + |b_1| \epsilon_1^{-p} \int_0^1 e^{-\mu x} |d^*(t,x)|^p dx \\ = & - \left[\mu \lambda_1 - |\kappa a| (p-1) \epsilon_0^{\frac{p}{p-1}} - |b_1| (p-1) \epsilon_1^{\frac{p}{p-1}} \right] V_1 + |\kappa a| \epsilon_0^{-p} \int_0^1 e^{-\mu x} |w(t,x)|^p dx \\ & + |b_1| \epsilon_1^{-p} \int_0^1 e^{-\mu x} |d^*(t,x)|^p dx. \end{aligned} \tag{A.20}$$

Next, using the comparison principle, we have, for all $x \in [0,1]$,

$$
\begin{aligned}
V_1(\bar{z}_3) \leq\ & e^{-[\mu\lambda_1-|\kappa a|(p-1)\epsilon_0^{\frac{p}{p-1}}-|b_1|(p-1)\epsilon_1^{\frac{p}{p-1}}]t}V_1(\bar{z}_3(0,\cdot)) \\
& + |\kappa a|\epsilon_0^{-p}\int_0^t e^{-[\mu\lambda_1-|\kappa a|(p-1)\epsilon_0^{\frac{p}{p-1}}-|b_1|(p-1)\epsilon_1^{\frac{p}{p-1}}](t-s)}ds\|w(s,\cdot)\|_{L^p}^p \\
& + |b_1|\epsilon_1^{-p}\int_0^t e^{-[\mu\lambda_1-|\kappa a|(p-1)\epsilon_0^{\frac{p}{p-1}}-|b_1|(p-1)\epsilon_1^{\frac{p}{p-1}}](t-s)}ds|d^*(s,\cdot)|_{L^p}^p. \qquad \text{(A.21)}
\end{aligned}
$$

Since $V_1(\bar{z}_3(0,x)) = 0$, for every $\varsigma > 0$, we obtain from (A21), the following estimate:

$$
\begin{aligned}
\|\bar{z}_3(t,\cdot)\|_{L^p} \leq\ & e^{\mu/p}\epsilon_1^{-1}\left(|b_1|\int_0^t e^{-\left[\mu\lambda_1-(|\kappa a|\epsilon_0^{\frac{p}{p-1}}+|b_1|\epsilon_1^{\frac{p}{p-1}})(p-1)-p\varsigma\right](t-s)}ds\right)^{1/p} \\
& \times \max_{0\leq s\leq t}\left(\|d^*(s,\cdot)\|_{L^p}e^{-\varsigma(t-s)}\right) \\
& + e^{\mu/p}\epsilon_0^{-1}\left(|\kappa a|\int_0^t e^{-\left[\mu\lambda_1-\left(|\kappa a|\epsilon_0^{\frac{p}{p-1}}+|b_1|\epsilon_1^{\frac{p}{p-1}}\right)(p-1)-p\varsigma\right](t-s)}ds\right)^{1/p} \\
& \times \max_{0\leq s\leq t}\left(\|w(s,\cdot)\|_{L^p}e^{-\varsigma(t-s)}\right). \qquad \text{(A.22)}
\end{aligned}
$$

Selecting

$$
\mu = \frac{p(|\kappa a|+|b_1|)\lambda_1/|b_1|+p\varsigma}{\lambda_1}, \qquad \text{(A.23)}
$$

and

$$
\epsilon_0 = \epsilon_1 = \left(\frac{\mu\lambda_1 p^{-1}-\varsigma}{|\kappa a|+|b_1|}\right)^{\frac{p-1}{p}} = \left(\frac{\lambda_1}{|b_1|}\right)^{\frac{p-1}{p}}, \qquad \text{(A.24)}
$$

we get from (A22) the following estimate:

$$
\begin{aligned}
\|\bar{z}_3(t,\cdot)\|_{L^p} \leq\ & e^{\left(\frac{|\kappa a|+|b_1|}{|b_1|}+\frac{\varsigma}{\lambda_1}\right)}(|b_1|)^{\frac{1}{p}}\left(\frac{\lambda_1}{|b_1|}\right)^{-\frac{p-1}{p}}\left(\int_0^t e^{-(|\kappa a|+|b_1|)\left(\frac{\lambda_1}{|b_1|}\right)(t-s)}ds\right)^{\frac{1}{p}} \\
& \times \max_{0\leq s\leq t}\left(\|d^*(s,\cdot)\|_{L^p}e^{-\varsigma(t-s)}\right)
\end{aligned}
$$

$$
\begin{aligned}
&+ e^{\left(\frac{|\kappa a|+|b_1|}{|b_1|}+\frac{\varsigma}{\lambda_1}\right)}(|\kappa a|)^{\frac{1}{p}}\left(\frac{\lambda_1}{|b_1|}\right)^{-\frac{p-1}{p}}\left(\int_0^t e^{-(|\kappa a|+|b_1|)\left(\frac{\lambda_1}{|b_1|}\right)(t-s)}ds\right)^{\frac{1}{p}}\\
&\times \max_{0\le s\le t}\left(\|w(s,\cdot)\|_{L^p}e^{-\varsigma(t-s)}\right)\\
\le& e^{\left(\frac{|\kappa a|+|b_1|}{|b_1|}+\frac{\varsigma}{\lambda_1}\right)}(|b_1|)^{\frac{1}{p}}\left(\frac{\lambda_1}{|b_1|}\right)^{-\frac{p-1}{p}}\left(\frac{|b_1|}{(|\kappa a|+|b_1|)\lambda_1}\right)^{\frac{1}{p}}\max_{0\le s\le t}\left(\|d^*(s,\cdot)\|_{L^p}e^{-\varsigma(t-s)}\right)\\
&+ e^{\left(\frac{|\kappa a|+|b_1|}{|b_1|}+\frac{\varsigma}{\lambda_1}\right)}(|\kappa a|)^{\frac{1}{p}}\left(\frac{\lambda_1}{|b_1|}\right)^{-\frac{p-1}{p}}\left(\frac{|b_1|}{(|\kappa a|+|b_1|)\lambda_1}\right)^{\frac{1}{p}}\max_{0\le s\le t}\left(\|w(s,\cdot)\|_{L^p}e^{-\varsigma(t-s)}\right). \qquad \text{(A.25)}
\end{aligned}
$$

Since

$$
\begin{aligned}
(|b_1|)^{\frac{1}{p}}\left(\frac{\lambda_1}{|b_1|}\right)^{-\frac{p-1}{p}}\left(\frac{|b_1|}{(|\kappa a|+|b_1|)\lambda_1}\right)^{\frac{1}{p}} &= (|b_1|)^{\frac{1}{p}}\left(\frac{\lambda_1}{|b_1|}\right)^{-1}\left(\frac{\lambda_1}{|b_1|}\right)^{\frac{1}{p}}\left(\frac{|b_1|}{(|\kappa a|+|b_1|)}\right)^{\frac{1}{p}}{\lambda_1}^{-\frac{1}{p}}\\
&\le (|b_1|)^{\frac{1}{p}}\left(\frac{\lambda_1}{|b_1|}\right)^{-1}\left(|b_1|\right)^{-\frac{1}{p}}{\lambda_1}^{\frac{1}{p}}(1)^{\frac{1}{p}}{\lambda_1}^{-\frac{1}{p}}\\
&\le \left(\frac{\lambda_1}{|b_1|}\right)^{-1} \qquad \text{(A.26)}
\end{aligned}
$$

and

$$
\begin{aligned}
(|\kappa a|)^{\frac{1}{p}}\left(\frac{\lambda_1}{|b_1|}\right)^{-\frac{p-1}{p}}\left(\frac{|b_1|}{(|\kappa a|+|b_1|)\lambda_1}\right)^{\frac{1}{p}} &= (|\kappa a|)^{\frac{1}{p}}\left(\frac{\lambda_1}{|b_1|}\right)^{-1}\left(\frac{\lambda_1}{|b_1|}\right)^{\frac{1}{p}}\left(\frac{1}{(|\kappa a|+|b_1|)}\right)^{\frac{1}{p}}\left(\frac{|b_1|}{\lambda_1}\right)^{\frac{1}{p}}\\
&= \left(\frac{\lambda_1}{|b_1|}\right)^{-1}\left(\frac{|\kappa a|}{(|\kappa a|+|b_1|)}\right)^{\frac{1}{p}}\\
&\le \left(\frac{\lambda_1}{|b_1|}\right)^{-1}, \qquad \text{(A.27)}
\end{aligned}
$$

according to (A25)–(A27), we have

$$
\begin{aligned}
\|\bar{z}_3(t,\cdot)\|_{L^p} \le& e^{\left(\frac{|\kappa a|+|b_1|}{|b_1|}+\frac{\varsigma}{\lambda_1}\right)}\frac{|b_1|}{\lambda_1}\max_{0\le s\le t}\left(\|d^*(s,\cdot)\|_{L^p}e^{-\varsigma(t-s)}\right)\\
&+ e^{\left(\frac{|\kappa a|+|b_1|}{|b_1|}+\frac{\varsigma}{\lambda_1}\right)}\frac{|b_1|}{\lambda_1}\max_{0\le s\le t}\left(\|w(s,\cdot)\|_{L^p}e^{-\varsigma(t-s)}\right). \qquad \text{(A.28)}
\end{aligned}
$$

Similarly, since $\bar{z}_4(0,x)$ also verifies (2.33), we get, for all $x\in[0,1]$,

$$
\begin{aligned}
\|\bar{z}_4(t,\cdot)\|_{L^p} &= \|\bar{z}_3(t,\cdot)\|_{L^p}\\
&\le e^{\left(\frac{|\kappa a|+|b_1|}{|b_1|}+\frac{\varsigma}{\lambda_1}\right)}\frac{|b_1|}{\lambda_1}\max_{0\le s\le t}\left(\left(\|d^*(s,\cdot)\|_{L^p}+\|w(s,\cdot)\|_{L^p}\right)e^{-\varsigma(t-s)}\right). \qquad \text{(A.29)}
\end{aligned}
$$

Using (A3) with (A12), (A14), (A28), (A29), and $p \to \infty$, it holds

$$\begin{aligned}\|z(t,\cdot)\|_\infty \le\ & e^{-\varsigma t} e^{\frac{\varsigma}{\lambda_1}} \|z(0,\cdot)\|_\infty \\ & + e^{\left(\frac{|\kappa a|+|b_1|}{|b_1|}+\frac{\varsigma}{\lambda_1}\right)\frac{2|b_1|}{\lambda_1}} \max_{\max\left\{0,t-\frac{1}{\lambda_1}\right\}\le s\le t} \left(\left(\|d^*(s,\cdot)\|_\infty + \|w(s,\cdot)\|_\infty\right) e^{-\varsigma(t-s)}\right) \\ & + e^{\frac{\varsigma}{\lambda_1}} |r| \max_{\max\left\{0,t-\frac{1}{\lambda_1}\right\}\le s\le t} \left(|w(s,0)| e^{-\varsigma(t-s)}\right). \end{aligned} \tag{A.30}$$

On the other hand, the explicit solution of (2.34) with dynamic boundary conditions (2.36)–(2.37) and initial data $w(0,x)$, $x \in [0,1]$ for all $t \in [0, \lim_{j\to\infty}(t_j))$, is given as follows:

$$w(t,x) = w\left(0, x+\lambda_2 t\right)\exp(-\kappa t) + \int_0^t \exp(-\kappa(t-\tau))(-b_2) d^*(\tau, x+\lambda_2 t - \lambda_2 \tau) d\tau, \tag{A.31}$$

for $0 \le t \le \frac{1-x}{\lambda_2}$, and

$$w(t,x) = \eta\left(t-\tfrac{1-x}{\lambda_2}\right)\exp\left(\tfrac{-\kappa}{\lambda_2}(1-x)\right) + \int_{t-\frac{1-x}{\lambda_2}}^t \exp(-\kappa(t-\tau))(-b_2) d^*(\tau, x+\lambda_2 t - \lambda_2 \tau) d\tau, \tag{A.32}$$

for $\frac{1-x}{\lambda_2} \le t$, with

$$\eta(t) = \exp(-\kappa t)\eta(0) - b_2 \int_0^t \exp(-\kappa(t-s)) d^*(s,1) ds. \tag{A.33}$$

From (A31) and (A32), the solution can be seen as the sum of the following terms for all $t \in [0, \lim_{j\to\infty}(t_j))$:

$$w(t,x) = \bar{w}_1(t,x) + \bar{w}_2(t,x) + \bar{w}_3(t,x), \tag{A.34}$$

where

$$\begin{aligned} \bar{w}_1(t,x) &:= w\left(0, x+\lambda_2 t\right)\exp(-\kappa t), \\ \bar{w}_2(t,x) &:= 0, \\ \bar{w}_3(t,x) &:= \int_0^t \exp(-\kappa(t-\tau))(-b_2) d^*(\tau, x+\lambda_2(t-\tau)) d\tau, \end{aligned} \tag{A.35}$$

for $t \in [0, \lim_{j\to\infty}(t_j))$, $x \in [0,1]$ with $0 \le t \le \frac{1-x}{\lambda_2}$, and

$$\begin{aligned} \bar{w}_1(t,x) &:= 0, \\ \bar{w}_2(t,x) &:= \eta\left(t-\tfrac{1-x}{\lambda_2}\right)\exp\left(\tfrac{-\kappa}{\lambda_2}(1-x)\right), \\ \bar{w}_3(t,x) &:= \int_{t-\frac{1-x}{\lambda_2}}^t \exp(-\kappa(t-\tau))(-b_2) d^*(\tau, x+\lambda_2(t-\tau)) d\tau, \end{aligned} \tag{A.36}$$

for $t \in [0, \lim_{j\to\infty}(t_j))$ with $\frac{1-x}{\lambda_2} \leq t$. We estimate the $L^p(0,1)$ norm of $\bar{w}_1$, with $p \in [1,\infty)$. Note that $\kappa > 0$ and from (A35)–(A36), the following estimate holds for every $\varsigma > 0$:

$$\begin{aligned}\left|\bar{w}_1(t,x)\right|^p &= \left|w\left(0, x+\lambda_2 t\right)\exp(-\kappa t)\right|^p \\ &\leq e^{-p\varsigma t}e^{p\varsigma\left(\frac{1-x}{\lambda_2}\right)}\left|w\left(0,x+\lambda_2 t\right)\right|^p \\ &\leq e^{-p\varsigma t}e^{p\varsigma\frac{1}{\lambda_2}}\left|w\left(0,x+\lambda_2 t\right)\right|^p, \end{aligned} \tag{A.37}$$

for all $t \in [0, \lim_{j\to\infty}(t_j)), x \in [0,1]$ with $0 \leq t \leq \frac{1-x}{\lambda_2}$. Therefore, we get

$$\left\|\bar{w}_1(t,\cdot)\right\|_{L^p} \leq e^{-\varsigma t}e^{\varsigma\frac{1}{\lambda_2}}\left\|w\left(0,\cdot\right)\right\|_{L^p}. \tag{A.38}$$

We estimate the $L^p(0,1)$ norm of $\bar{w}_2$, with $p \in [1,\infty)$. From (A35)–(A36), the following estimate holds for every $\varsigma > 0$ and $\kappa > 0$:

$$\begin{aligned}\left|\bar{w}_2(t,x)\right|^p &= \left|\eta\left(t-\tfrac{1-x}{\lambda_2}\right)\exp\left(\tfrac{-\kappa}{\lambda_2}(1-x)\right)\right|^p \\ &\leq e^{p\varsigma\frac{x}{\lambda_2}}e^{-p\varsigma\frac{1}{\lambda_2}}e^{-p\varsigma\left(\left(t-\left(t+\frac{1-x}{\lambda_2}\right)\right)\right)}\left|\eta\left(t-\tfrac{1-x}{\lambda_2}\right)\right|^p \\ &\leq e^{p\varsigma\frac{x}{\lambda_2}}\max_{t-\frac{1-x}{\lambda_2}\leq s\leq t}\left(|\eta(s)|^p e^{-p\varsigma(t-s)}\right) \\ &\leq e^{p\varsigma\frac{x}{\lambda_2}}\max_{\max\{0,t-\frac{1}{\lambda_2}\}\leq s\leq t}\left(|\eta(s)|^p e^{-p\varsigma(t-s)}\right). \end{aligned} \tag{A.39}$$

Hence, we obtain for every $\varsigma > 0, p \in [1,\infty)$ and $t \geq 0$

$$\left\|\bar{w}_2(t,\cdot)\right\|_{L^p} \leq e^{\varsigma\frac{1}{\lambda_2}}\max_{\max\left\{0,t-\frac{1}{\lambda_2}\right\}\leq s\leq t}\left(|\eta(s)|\, e^{-\varsigma(t-s)}\right). \tag{A.40}$$

Using Lyapunov analysis, we estimate the $L^p(0,1)$ norm of $\bar{w}_3$, with $p \in [1,\infty), \sigma > 0$. We have $\bar{w}_3(t,1) = 0$ for $t \in [0, \lim_{j\to\infty}(t_j))$.

Let us define

$$V_2(\bar{w}_3) = \int_0^1 e^{\sigma x}|\bar{w}_3(t,x)|^p dx. \tag{A.41}$$

We compute the time derivative of $V_2(\bar{w}_3)$ as follows:

$$\begin{aligned}\dot{V}_2(\bar{w}_3) &= p\int_0^1 e^{\sigma x}sign(\bar{w}_3(t,x))\bar{w}_{3t}(t,x)|\bar{w}_3(t,x)|^{p-1}dx \\ &= p\int_0^1 e^{\sigma x}sign(\bar{w}_3(t,x))\left[\lambda_2\bar{w}_{3x}(t,x) - \kappa\bar{w}_3(t,x) - b_2 d^*(t,x)\right]|\bar{w}_3(t,x)|^{p-1}dx. \end{aligned} \tag{A.42}$$

Since

$$p\int_0^1 e^{\sigma x} sign(\bar{w}_3(t,x))\lambda_2 \bar{w}_{3x}(t,x)|\bar{w}_3(t,x)|^{p-1}dx = \lambda_2\left[e^{\sigma x}|\bar{w}_3(x)|^p\right]_0^1 - \int_0^1 e^{\sigma x}\sigma\lambda_2|\bar{w}_3(x)|^p dx$$
$$= \lambda_2 e^{\sigma}|\bar{w}_3(1)|^p - \lambda_2|\bar{w}_3(0)|^p - \sigma\lambda_2\int_0^1 e^{\sigma x}|\bar{w}_3(x)|^p dx \tag{A.43}$$

and

$$|\bar{w}_3(x)|^{p-1}d^*(t,x) \le \frac{p-1}{p}\epsilon_2^{\frac{p}{p-1}}|\bar{w}_3(x)|^p + \frac{1}{p}\epsilon_2^{-p}|d^*(t,x)|^p, \tag{A.44}$$

substituting (A43)–(A44) into (A42), we get

$$\begin{aligned}\dot{V}_2(\bar{w}_3) &\le \lambda_2 e^{\sigma}|\bar{w}_3(1)|^p - \lambda_2|\bar{w}_3(0)|^p - \sigma\lambda_2 V_2(\bar{w}_3) - p\kappa V_2(\bar{w}_3)\\ &\quad + (p-1)|b_2|\epsilon_2^{\frac{p}{p-1}}V_2(\bar{w}_3) + |b_2|\epsilon_2^{-p}\int_0^1 e^{\sigma x}|d^*(t,x)|^p dx\\ &\le -\left(\sigma\lambda_2 + p\kappa - (p-1)|b_2|\epsilon_2^{\frac{p}{p-1}}\right)V_2(\bar{w}_3) + |b_2|\epsilon_2^{-p}\int_0^1 e^{\sigma x}|d^*(t,x)|^p dx\\ &\le |b_2|\epsilon_2^{-p}e^{\sigma}\|d^*(t,x)\|_{L^p}^p - \left(\sigma\lambda_2 + p\kappa - (p-1)|b_2|\epsilon_2^{\frac{p}{p-1}}\right)V_2(\bar{w}_3).\end{aligned} \tag{A.45}$$

Using the comparison principle and the fact that $V_2(0) = 0$ (since $\bar{w}_3(0,x) = 0$), we get for all $t \in [0, \lim_{j\to\infty}(t_j)), x \in [0,1]$

$$\begin{aligned}V_2(\bar{w}_3) &\le |b_2|\epsilon_2^{-p}e^{\sigma}\int_0^t e^{-(\sigma\lambda_2 + p\kappa - (p-1)|b_2|\epsilon_2^{\frac{p}{p-1}})(t-s)}\|d^*(s,\cdot)\|_{L^p}^p ds\\ &\le |b_2|\epsilon_2^{-p}e^{\sigma}\int_0^t e^{-(\sigma\lambda_2 + p\kappa - (p-1)|b_2|\epsilon_2^{\frac{p}{p-1}} - p\varsigma)(t-s)}ds \max_{0\le s\le t}\left(\|d^*(s,\cdot)\|_{L^p}^p e^{-p\varsigma(t-s)}\right).\end{aligned} \tag{A.46}$$

Thus, we have

$$\|\bar{w}_3(t,\cdot)\|_{L^p} \le \left(|b_2|\int_0^t e^{-(\sigma\lambda_2 + p\kappa - (p-1)|b_2|\epsilon_2^{\frac{p}{p-1}} - p\varsigma)(t-s)}ds\right)^{1/p} e^{\sigma/p}\epsilon_2^{-1}\max_{0\le s\le t}\left(\|d^*(s,\cdot)\|_{L^p}e^{-\varsigma(t-s)}\right). \tag{A.47}$$

Selecting

$$\sigma = \frac{p\lambda_2 - p\kappa + p\varsigma}{\lambda_2} \tag{A.48}$$

and

$$\epsilon_2 = \left(\frac{\sigma\lambda_2 p^{-1} + \kappa - \varsigma}{|b_2|}\right)^{\frac{p-1}{p}} = \left(\frac{\lambda_2}{|b_2|}\right)^{\frac{p-1}{p}}, \tag{A.49}$$

we get

$$\|\bar{w}_3(t,\cdot)\|_{L^p} \le e^{\left(1-\frac{\kappa}{\lambda_2}+\frac{\varsigma}{\lambda_2}\right)}\left(\frac{\lambda_2}{|b_2|}\right)^{-\frac{p-1}{p}}|b_2|^{\frac{1}{p}}\left(\int_0^t e^{-(p\lambda_2-(p-1)\lambda_2)(t-s)}ds\right)^{1/p}\max_{0\le s\le t}\|d^*(s,\cdot)\|_{L^p}e^{-\varsigma(t-s)}$$

$$\le e^{\left(1-\frac{\kappa}{\lambda_2}+\frac{\varsigma}{\lambda_2}\right)}\left(\frac{\lambda_2}{|b_2|}\right)^{-\frac{p-1}{p}}|b_2|^{\frac{1}{p}}\left(\frac{1}{\lambda_2}\right)^{\frac{1}{p}}\max_{\max\left\{0,t-\frac{1}{\lambda_2}\right\}\le s\le t}\|d^*(s,\cdot)\|_{L^p}e^{-\varsigma(t-s)}. \tag{A.50}$$

Since the following holds:

$$\left(\frac{\lambda_2}{|b_2|}\right)^{-\frac{p-1}{p}}|b_2|^{\frac{1}{p}}\left(\frac{1}{\lambda_2}\right)^{\frac{1}{p}} = \left(\frac{\lambda_2}{|b_2|}\right)^{-1}\left(\frac{\lambda_2}{|b_2|}\right)^{\frac{1}{p}}\left(\frac{|b_2|}{\lambda_2}\right)^{\frac{1}{p}}$$

$$= \left(\frac{\lambda_2}{|b_2|}\right)^{-1}, \tag{A.51}$$

substituting (A51) into (A50), we have

$$\|\bar{w}_3(t,\cdot)\|_{L^p} \le e^{\left(1-\frac{\kappa}{\lambda_2}+\frac{\varsigma}{\lambda_2}\right)}\left(\frac{\lambda_2}{|b_2|}\right)^{-1}\max_{\max\left\{0,t-\frac{1}{\lambda_2}\right\}\le s\le t}\|d^*(s,\cdot)\|_{L^p}e^{-\varsigma(t-s)}. \tag{A.52}$$

Using (A34) with (A38), (A40), (A52), and $p\to\infty$, it holds

$$\|w(t,\cdot)\|_\infty \le e^{-\varsigma t}e^{\frac{\varsigma}{\lambda_2}}\|w(0,\cdot)\|_\infty + \frac{|b_2|}{\lambda_2}e^{\left(1-\frac{\kappa}{\lambda_2}+\frac{\varsigma}{\lambda_2}\right)}\max_{\max\left\{0,t-\frac{1}{\lambda_2}\right\}\le s\le t}\|d^*(s,\cdot)\|_\infty e^{-\varsigma(t-s)}$$

$$+ e^{\frac{\varsigma}{\lambda_2}}\max_{\max\left\{0,t-\frac{1}{\lambda_2}\right\}\le s\le t}|\eta(s)|e^{-\varsigma(t-s)}. \tag{A.53}$$

The proof is complete.